Late Holocene Climate and Glacier Fluctuations in the Cambria Icefield area, British Columbia Coast Mountains

by

Kate Johnson
BSc, Lancaster University, 2008

A Thesis Submitted in Partial Fulfillment
of the Requirements for the Degree of

MASTER OF SCIENCE

in the Department of Geography

Supervisory Committee

Late Holocene Climate and Glacier Fluctuations in the Cambria Icefield area, British Columbia Coast Mountains

by

Kate Johnson
BSc, Lancaster University, 2008

Supervisory Committee

Dr. Dan J. Smith, (Department of Geography)
Supervisor

Dr. Terri Lacourse (Department of Geography)
Departmental Member

Abstract

Supervisory Committee

Supervisor
Dr. Dan J. Smith, (Department of Geography)

Departmental Member
Dr. Terri Lacourse (Department of Geography)

In the British Columbia Coast Mountains most dendroclimatological and dendroglaciological studies have focused on developing insights from tree-ring sites located in the southern and central regions. By contrast relatively few studies have been conducted in the northwestern Coast Mountains, where exploratory studies reveal that significant climate-radial growth relationships exist. The purpose of this study was to develop a proxy record of climate change from tree rings and to reconstruct the late Holocene glacial history of two outlet glaciers spilling eastward from the Cambria Icefield.

Dendroclimate investigations were conducted using mountain hemlock (*Tsuga mertensiana*) trees growing on three high-elevation montane slopes. The three stands located along a 35 km transect cross date to form a master chronology for the region spanning 409 years (1596 to 2007 A.D.). Correlation analyses show that the radial growth of the regional tree-ring chronology corresponds to variations in the mean June-July-August (JJA) air temperature. The relationship between the two variables was used to reconstruct mean JJA air temperature from 1680 to 2007 A.D.). The reconstruction illustrates warm and cool intervals that are synchronous

to those derived from other paleoenvironmental research in this region. The proxy record also highlights annual to inter-decadal climate variability likely resulting from atmospheric-ocean circulation patterns described by the El Niño-Southern Oscillation and the Pacific Decadal Oscillation.

The late Holocene behaviour of White and South Flat glaciers was investigated using radiocarbon dating techniques, dendrochronological cross-dating techniques and geomorphological analysis of sedimentary units within the White and South Flat glacier forefields. Evidence for a First Millennial Advance (FMA) cumulating around 650 A.D. and early Little Ice Age (LIA) advances at 1200 and 1400 A.D. were documented. These advances are contemporaneous with the late Holocene activity of glaciers throughout the region, suggesting coherent broad-scale climate forcing mechanisms have influence glacial mass balance regimes over at least the last two millennia.

The dendroclimatological and dendroglaciological findings of the study provide the first annually-resolved climate record for the region and help to enhance our understanding of late-Holocene glacier behaviour in the Cambria Icefield Area. The thesis documents the complex interactions between climate and the radial growth of mountain hemlock trees in the Pacific Northwest, and describes the role that long-term climate variability played in glacier dynamics during the FMA and LIA.

Table of Contents

List of Tables

List of Figures

Acknowledgments

First and foremost, to Dan Smith: your patience with my "early" rising (at 9am) in the field, guidance down Jambeau Glacier's crevasses, enthusiasm for grizzly bears in the Coast Mountains, and love for earthquakes in the 1700s has been second to none. Those sleepless nights wondering if I had a granola bar in my bag couldn't have been completed without you!

Thank you also to Terri Lacourse, whose speedy edits have improved this thesis in ways I couldn't have achieved, even after the 100th attempt.

The field work couldn't have been completed without the Midnight Dream and Knight Rider gangs. Thanks for all the hazy memories involving Hyderizing, karaoke, KAJOs and pie (man, I love me some pie). And thank you to all the lovely ladies I met back at the "VicTree" lab.

To my friends, whether in the UK or Canada, I appreciate your support throughout this adventure, and to my family, for your understanding on why I was 5,000 miles away and still complaining about the Northampton Town score.

Last but by no means least, I thank kypp; I'll be indebted to your patience and attempt at understanding my frustrations over cross dating and statistics. For this, I probably owe you a few dinners at the Ramore. And also for those immortal words: "wait, so, Dendrochro- whatsit is a real word?"

Chapter 1

Introduction

1.1 Introduction

The global climate is undergoing substantive changes that are resulting in fundamental shifts in climate patterns which could significantly impact our society and ecosystems (Mann *et al*. 1999). To fully understand the nature and character of these changes, it is essential that we develop an understanding of past climate conditions and place these historical changes into a longer temporal context (Hansen and Lebedeff 1987). Due to limitations in the length and distribution of instrumental climatic records, high-resolution multi-proxy methods have proven critical in providing the insights needed to interpret current climate trends and to establish long-term ranges of variability (Black *et al.* 2009). Prior and ongoing research suggests that tree-rings provide the kind of annually resolved insights that are necessary for extending climatic records back several millennia (D'Arrigo *et al*. 2005).

The science of dendrochronology (or tree-ring studies) has focused on the annual growth rings of temperate zone trees to establish the date and chronological order of past events (Fritts 1976). Tree-ring chronologies can be dendroclimatically interpreted to reconstruct a variety of environmental variables when correlated with instrumental data or records (Cook and Kairiukstis 1990). While long-lived tree species provide annually-resolved chronologies that can extend back as far as 3,000 years, subfossil wood samples have been employed to

extend tree-ring and proxy climate records back through the Holocene (Grudd *et al*. 2002).

Dendroclimatology is the science that uses tree-rings to study present climate and reconstruct past climate (Luckman 2007). This methodology allows dendrochronologists to place existing short instrumental climate records in a longer temporal context, and allows for comparison of the spatial patterns of climate change. In Pacific North America Holocene regional-scale climate changes are known to directly impact upon the mass balance state of glaciers resulting in sustained periods of expansion and retreat (Reyes *et al*. 2006).

Dendroglaciology is a branch of dendrochronology that uses tree-rings to study and date the response of glaciers to changing climates (Luckman 1986). It allows for the development of long-term tree-ring chronologies for dating events over large areas, and hence for examination of the synchronicity of glacier activity at different time scales (Luckman and Villalba 2001). Applied dendroglaciological research has successfully established a link between glacier mass balance and tree-ring-width variability (Smith and Lewis 2007a).

In the Coast Mountains of British Columbia (B.C.), prior dendroclimatological and dendroglaciological studies have primarily focused on developing insights at tree-ring sites located in the southern and central regions (e.g., Larocque and Smith 2003; Allen and Smith 2007). By contrast relatively few tree-ring studies have been conducted in the north Coast Mountains, where exploratory studies by Penrose (2007) and Jackson *et al*. (2008) revealed that significant climate-radial growth relationships do exist. The purpose of this study

was to reconstruct the environmental history of the Cambria Icefield area. Specific attention was given to developing a proxy record of climate change and to reconstructing the late Holocene glacial history of two outlet glaciers spilling eastward from the icefield. The overarching intent was to determine whether the late Holocene climate and glacier fluctuations in this regional are similar to those recorded in the central and southern Coast Mountains.

1.2 Research Objectives

The research had three specific objectives:

1. to develop a proxy record of climate change from tree ring-width chronologies collected in the vicinity of the Cambria Icefield.
2. to describe the late Holocene glacial history of White and South Flat glaciers in the Cambria Icefield.
3. to investigate the long-term glaciological response of White and South Flat glaciers to changing climates .

1.3 Thesis Format

Chapter 2 presents the findings of a dendroclimatological reconstruction from tree-ring records collected at sites in the vicinity of the Cambria Icefield. Chapter 3 describes the dendroglaciological findings from field investigations completed at White and South Flat glaciers. Chapters 2 and 3 are formatted as manuscripts prepared for submission to refereed journals. Chapter 4 provides an overview of the findings of the research, and considers the relationship between long-term climate changes and glaciological behaviour of the White and South Flat

glaciers. The chapter concludes with a presentation of the limitations study and provides recommendations for future research.

Chapter 2

A 323-year dendroclimatic reconstruction of summer mean air temperature in the northern British Columbia Coast Mountains, Canada

2.1 Introduction

Climate plays an important role in limiting the annual radial growth of montane trees in the British Columbia (B.C.) Coast Mountains (e.g., Gedalof and Smith 2001a; Larocque and Smith 2004; Parish and Antos 2006). Previous studies in the region highlight a correlation between apical growth and environmental factors such as summer growing season temperature, previous growth year temperature, and spring snowpack depth (Larocque and Smith 2004). The year-to-year correlation of tree rings to these seasonal climate variables indicates these trees have considerable potential for constructing dendroclimatic proxy records (Luckman 2007).

In Pacific North America (PNA) mountain hemlock (*Tsuga mertensiana* [Bong.] Carr.) trees are widely dispersed, covering a latitudinal range extending from southern Alaska to northern California (Krajina 1969; Means 1990). In B.C. the mountain hemlock zone occupies elevations between 900 to 1800 m asl in the south (lower on windward slopes, higher on leeward slopes), and 400 to 1000 m asl in the north (Pojar *et al.* 1987). Dendroclimatological analyses show that mountain hemlock trees are sensitive recorders of annual changes in high elevation climates (Laroque and Smith 2001). Researchers have shown that their

radial growth is conditioned by a limited number of climate stressors depending upon their location (Graumlich and Brubaker 1986; Gedalof and Smith 2001b). These climate-radial growth relationships have been used to construct proxy models of past climates using both single chronologies and regional networks of chronologies (i.e., Wiles *et al*. 1998; Gedalof and Smith 2001b).

The goal of the research presented in this chapter was to construct an annually-resolved proxy record of climate change in the northwestern Coast Mountains. The intent was to quantify the climate-radial growth associations displayed by living mountain hemlock stands found growing in close proximity to the Cambria and Todd icefields. Historic climate station data was compared to the total ring-width growth trends over the period of record and used to construct a proxy record of climate extending back over the extent of the tree-ring record. The proxy reconstruction was compared to several climate indices to reveal which forcing mechanisms may have interacted to define the regional climate over the last 300 years.

2.2 Research Background

2.2.1 Climate forcing in the Pacific Northwest

The Coast Mountains flank the western coastline of B.C. (Figure 2.1). This high mountain landscape extends for ca. 1600 kms from the northwestern corner of the province southward to close to the international border with Washington State (Means 1990). The climate of the region is moderated by proximity to the Pacific Ocean (Mantua *et al.* 1997), with inter- annual to inter-decadal variability

Figure 2.1: Location of the sample sites and climate stations used in this thesis.

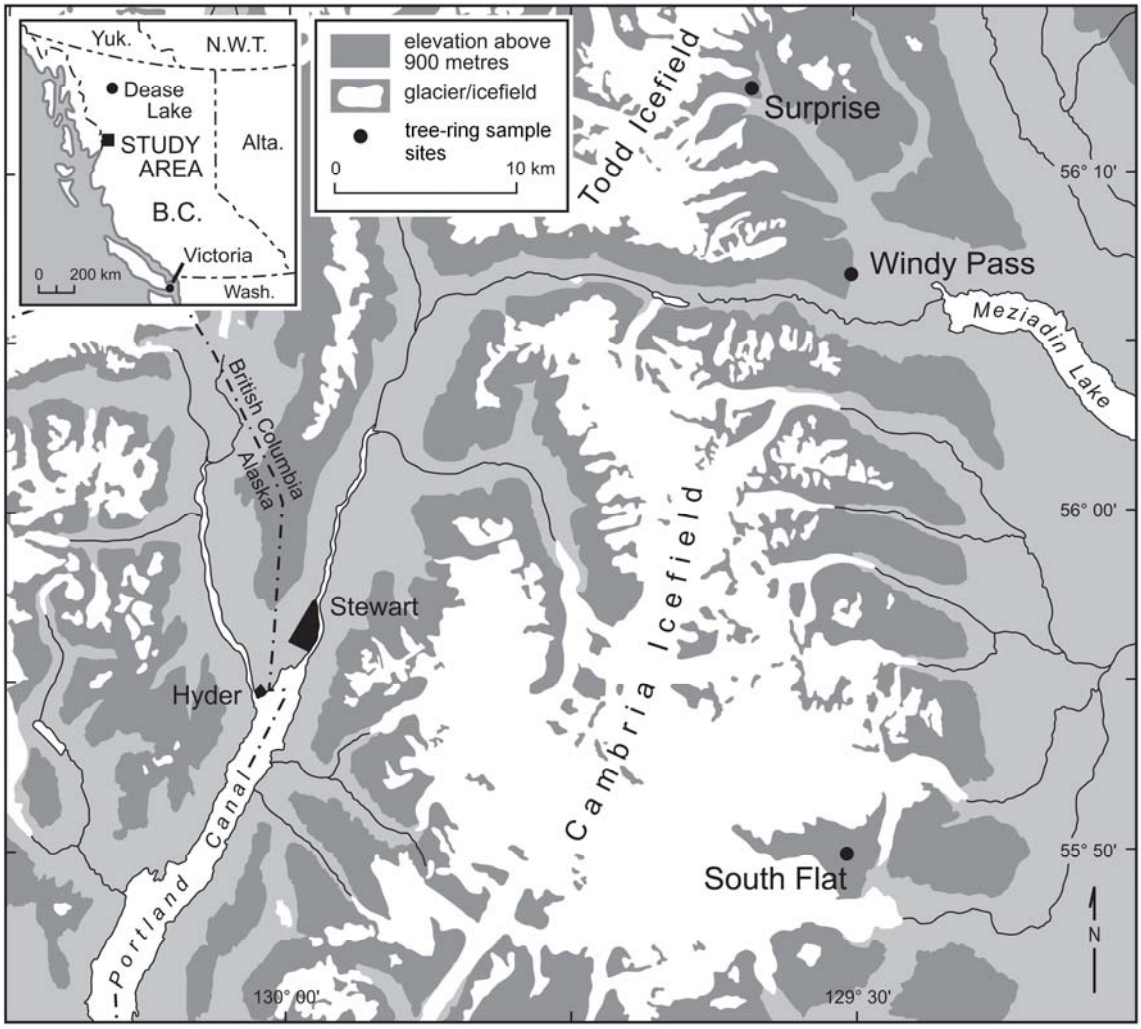

largely resulting from atmospheric-ocean circulation patterns described by the El Niño South Oscillation (ENSO) and the Pacific Decadal Oscillation (PDO; Bonsal *et al.* 2001).

ENSO describes the influence of both ocean and atmospheric circulation patterns in PNA (Rasmussan and Wallace 1983). It is widely accepted as representative of the climate forcing parameters that lead to hemispheric-scale inter-annual climate variations (Mantua and Hare 2002). Periodic shifts in the strength of ENSO result in weather and climate anomalies every 7 to 10 years (Rasmussan and Wallace 1983). In the Coast Mountains, ENSO events are generally correlated to anomalously warmer and drier winter months (Bonsal *et al*. 2001).

The PDO is a long-term El Niño-like ocean and atmospheric circulation pattern that occurs in the Northern Pacific, with a positive (or warm) phase or a negative (or cool) phase (Manuta and Hare 2001). It is known to change phases with an abrupt step-like shift in mean winter sea level pressure (Trenberth 1990; Mantua and Hare 2002). Climate anomalies associated with positive (or warm) phases coincide with anomalously warmer and wetter periods in PNA (Mantua and Hare 2002).

Three PDO shifts in the past century resulted in "cool" phases from 1890 to 1924, and again from 1947 to 1976; and, "warm" phases from 1925 to 1946 and from 1977 to the mid-1990s (Mantua *et al.* 1997). Tourre *et al.* (2001) indicate that the PDO has an interdecadal mode of between 12 to 25 years and a decadal mode of between 9 to 12 years. Gedalof and Smith (2001b) employed dendrochronological methods to construct a proxy record of spring PDO conditions

over the last 400 years. Their reconstruction illustrates the long-term average duration between PDO shifts is 23 years.

2.2.2 Dendroclimatology of mountain hemlock

Previous research established that mountain hemlock trees are a useful species for dendroclimatic studies due to their spatial range and sensitivity to climate (Gedalof 2002; Penrose 2007). Generally, mountain hemlocks are found at locations characterized by cool, wet climates and deep winter snowpacks (Peterson and Peterson 2001). Annual radial growth increment of mountain hemlock has been correlated with mean summer temperature (Gedalof and Smith 2001a), winter precipitation described by spring snowpack depth (Graumlich and Brubaker 1986; Gedalof and Smith 2001a; Peterson and Peterson 2001) and April precipitation totals (Penrose 2007).

2.3 Location

Sampling was undertaken at sites located in close proximity to the Todd and Cambria icefields (Figure 2.1). This glaciated high mountain region is characterized by topographic relief exceeding 900 m (Figure 2.1). The local tree line is found at ca. 1500 m asl, significantly above the present-day terminus of glaciers in the region at ca. 1200 m asl (Laxton 2005; Jackson *et al.* 2008).

Montane forests in this region of the Coast Mountains consist of single-species stands of mountain hemlock or co-dominant stands of mountain hemlock and subalpine fir (*Abies lasiocarpa* [Hook.] Nutt.). Mountain hemlock forests

typically have a dense shrub growth under the tree canopy, with thick carpet of moss covering the forest floor (Klinka *et al.* 1991).

Adjusted and Homogenized Canadian Climate Data (AHCCD) data indicate the montane forests in the vicinity of Stewart are characterized by warm, wet conditions with mean annual temperatures of 5.6°C, and annual total precipitation of 1458 mm(Environment Canada 2009). The eastern slopes of the Coast Mountains in the vicinity of the Cambria and Todd icefields experience drier and cooler conditions with mean annual temperatures of -0.9°C, and annual total precipitation of 292 mm (Environment Canada 2009).

2.3.1 Study Sites

Samples were collected from three mountain hemlock stands found along a 35 km north to south transect (Figure 2.1). The sampling sites are located close to the easternmost extent of mountain hemlocks in the region (Pojar *et al.* 1987; Klinka *et al.* 2001).

The northernmost site is located in the headwaters of Surprise Creek at 910 m asl (Lat 56° 12’ N, Long 129° 36’ W; Figure 2.1). Positioned on a moderately sloped forested ridge line between the recently deglaciated forefields of Surprise Glacier (*unofficial name*) to the south and an unnamed glacier to the north, the mature mountain hemlock trees (<6 m tall) found at the site were intermixed with mature subalpine firs whose maximum age exceeded 355 years (Jackson *et al.* 2008).

The Windy Pass site (Lat 56° 06' N, Long 129° 30' W; Figure 2.1) is located 8.6 km east of Bear Pass above the Stewart-Cassier Highway (Highway 37) close to the upper altitudinal extent of standing trees. Located on a southerly-facing minor bench at 1090 m asl, 11 km southeast of the Surprise site, the forest at Windy Pass site is dominated by short stature (<4 m) mature mountain hemlock trees (Figure 2.2).

Figure 2.2: The Windy Pass Site at 1080 m asl, with a Remote Avalanche Weather Stations (RAWS) used for avalanche prediction in the region. Photo: Dan Smith.

The South Flat site (Lat 55° 49' N, Long 129° 29'; 1035 m asl; Figure 2.1) is located on a steep southeast-facing forested site at 1035 m asl in close proximity to White Glacier (*unofficial name*), approximately 33 km south of the Windy Pass site.

The site is dominated by a mature even-aged mountain hemlock forest (>6 m height) and contains scattered subalpine fir (Figure 2.3).

Figure 2.3: The South Flat Site located west of South Flat Glacier at 1035 m asl. Trees were growing on a south-east facing slope dominated by mountain hemlock trees and scattered with subalpine fir. Photo: Dan Smith.

2.4 Methodology

2.4.1 Dendrochronology

Tree ring samples were collected from mature trees with no obvious signs of crown damage or butt rot. Samples were collected at breast height with 18" increment borers using standard dendrochronological techniques (Stokes and Smiley 1964). Two increment cores ≥90° apart were extracted from each tree to

pith and stored in plastic straws for transport to the University of Victoria Tree Ring Laboratory.

The cores were allowed to air-dry, glued into slotted mounting boards, and sanded with progressively finer sandpaper to a 600-grit polish (Stokes and Smiley 1968). Ring widths were measured to the nearest 0.01 mm along a single radius using WinDendro software and a high resolution flatbed scanner (Guay *et al*. 1992). For series with exceptionally narrow annual rings, the ring widths were measured with MeasureJ2X software (VoorTech Consulting 2009) to the nearest 0.01 mm using a Velmex-stage equipped with a microscope, CCD video display and Metronics QC-10V digital readout.

Each ring-width series was first visually cross dated by comparing narrow marker rings with CDendro software (Cybis Elektronic & Data AB). Following this the International Tree Ring Database (ITRDB) software program COFECHA was used to verify the cross dating using block correlations between each tree series and the master chronology (Holmes *et al*. 1986). COFECHA correlations were calculated using a 50-year segment length lagged successively by 25 years at a one-tailed 99% confidence level (Grissino-Meyer 2001). Ring width series with anomalous growth patterns not significantly correlated to the group were removed from the data set.

A regional master chronology was created by combining and cross dating the three individual chronologies. Any ring width series that did not significantly correlate to the master chronology was removed from the data set to allow for the strongest possible series intercorrelation.

All of the ring width series within the master chronology were transformed into stationary, dimensionless indices to remove growth trends related to tree age and stand dynamics (Cook 1985). The indices were established using double detrending options in the IITRDB software program ARSTAN (Cook and Holmes 1986) to retain any low-frequency variability within the resulting chronology (Cook *et al*. 1990). Initially a best-fit negative exponential curve or linear trend line was fitted to each individual series. Each observed ring width in the series was then divided by this value. Following this, the individual cores were detrended a second time by fitting a cubic smoothing spline with a 50% frequency cutoff of 95 years (Cook and Peters 1981). To create a single dimensionless value for each growth year, each ring-width-index series was prewhitened using autoregressive and moving average models to remove any autocorrelation effects (Cook 1985; Biondi and Swetnam 1987). A robust mean was then used to combine the detrended series from each site into residual master site chronology (Fritts 1976).

To ensure robust signal strength through time, each site chronology and the master chronology was terminated at an established "expressed population signal" (EPS) value (Wigley *et al*. 1984). EPS values were calculated for 25-year moving periods to quantify signal strength through time; the cut-off year was defined as the central year within the last 25-year segment where the EPS value was greater than the 0.85 cut-off value (Wilson and Luckman 2002).

Bootstrapped correlation and response function analyses were undertaken to evaluate the climate-radial growth response of the chronologies using the software program DENDROCLIM2002 (Biondi and Waikul 2004). Climate variables

were compared to the residual chronologies using bootstrap correlations. The stability of the climate influence on radial growth was analysed by calculating block correlations of 30 years duration with an overlap of 15 years.

After determining which climate variable was significantly correlated to the master chronology, a linear regression model was used to represent the proxy relationship between ring width and climate using the most recent 50% of the data (LeBlanc and Terrell 2001; Hughes 2002). A split period verification analysis and a simple Pearson's correlation were used to verify the linear regression model's ability to represent the remaining 50% of historic data (Fritts 1976). Following this procedure, the model was invoked over the duration of the residual master chronology to illustrate climate variability through time.

2.4.2 Climate Data

Mean, maximum, and minimum monthly temperature and precipitation data were obtained from the AHCCD website (http://www.cccma.ec.gc.ca/hccd/). Missing values were replaced with long-term monthly averages.

Only two climate stations in the region have lengthy historical records. The closest to the sampling sites is located at the Stewart Airport (Climate Station 1067742; Lat 55° 56′ N, Long 129° 59′ W; Figure 2.1). Located on the windward side of the Cambria Icefield at 7 m asl, the station experiences a coastal maritime climate and has been operational since 1911. The annual air temperature averages 5.6°C, with the coldest month (January) averaging –3.7°C and the warmest (July)

15.1°C (Environment Canada 2009). The total annual precipitation at Stewart averages 1843 mm, with more than 30% of this falling as snow.

The nearest climate station located on the leeward side of the Boundary Range is found at Dease Lake, approximately 260 km northeast of the Surprise site (Climate station 1182285; Lat 58° 43' N; Long 130° 02' W; Figure 2.1). The station is located at 807 m asl and has been operational since 1944. The annual air temperature averages -0.9°C, with the coldest month averaging -14.2°C and the warmest 12.2°C (Environment Canada 2009).

Historical sea surface temperature (SST) records provide insights into the role that climate forcing events associated with the PDO and ENSO have on radial growth (D'Arrigo *et al*. 1999). The Hadley Centre's HADISST's global gridded 1° Latitude x 1° Longitude mean monthly SST from 1870 to present were used as a surrogate for PDO and ENSO phases. This data was correlated with the master chronology using the interactive KNMI climate explorer website (http://climexp.knmi.nl; van Oldenborgh and Burgers 2005).

To understand the temporal rhythm of these climate forcing events on the radial growth of mountain hemlock trees, an interactive web-based wavelet analysis[1] was employed. In this instance, a Gaussian 2 function was used as the base function with a 5% white noise reduction.

[1] http://paos.colorado.edu/research/wavelets; (Torrence and Compo 1998)

2.5 Results

2.5.1 Tree-ring chronologies

Twenty-six ring width series from 20 trees were included in the chronology from the Surprise site. The final chronology spans 409 years (1596 to 2007), with an EPS cut off at 1680. The ring width series has a mean inter-series correlation of 0.535 and an average mean sensitivity of 0.211 (Table 2.1).

Table 2.1: Tree-ring chronology statistics.

Site	Latitude	Longitude	Elevation (m asl)	Series mean first-order autocorrelation[a]	Series mean sensitivity[b]	Total series length (years)
Surprise	56° 12’	129° 36’	910	0.535	0.211	408
Windy Pass	56 ° 06’	129° 30’	1090	0.595	0.271	391
South Flat	55°49’	129° 29’	1035	0.548	0.231	373
Master	-	-	-	0.544	0.244	411

[a] a measure of the strength of the signal (typically the climate signal) common to all sampled trees at the site (Grissino-Mayer 2001)

[b] a measure of the relative change in ring-width from one year to the next in a given series (Grissino-Mayer 2001)

Thirty-six ring width series from 23 individual trees were included in the final analysis of increment cores collected at the Windy Pass site. The site chronology spans 391 years (1613 to 2004), with an EPS cut off at 1730 due to a limited sample depth beyond this. The ring width series have a mean inter-series correlation of 0.595 and a mean sensitivity of 0.271 (Table 2.1).

Twenty-seven ring width series from 17 individual trees were included in the final analysis of samples from the South Flat site, the site chronology spans 373 years (1635 to 2007), with an EPS cut off at 1700. The ring width series have a mean inter-series correlation of 0.548 and a mean sensitivity of 0.231 (Table 2.1).

The site chronologies strongly correlate to one another (Figure 2.4). While the radial growth trends between the South Flat and Windy Pass sites are strongly

Figure 2.4: The residual tree-ring chronologies for (a) Surprise, (b) Windy Pass, and (c) South Flat sites with a 10 year running mean.

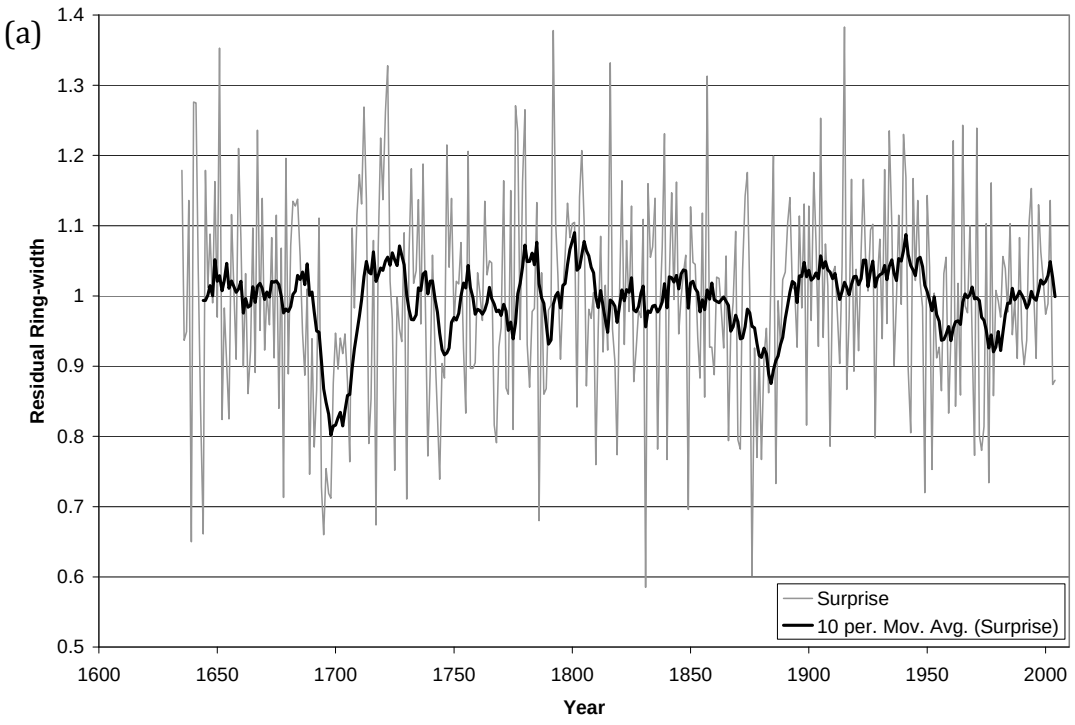

(b)

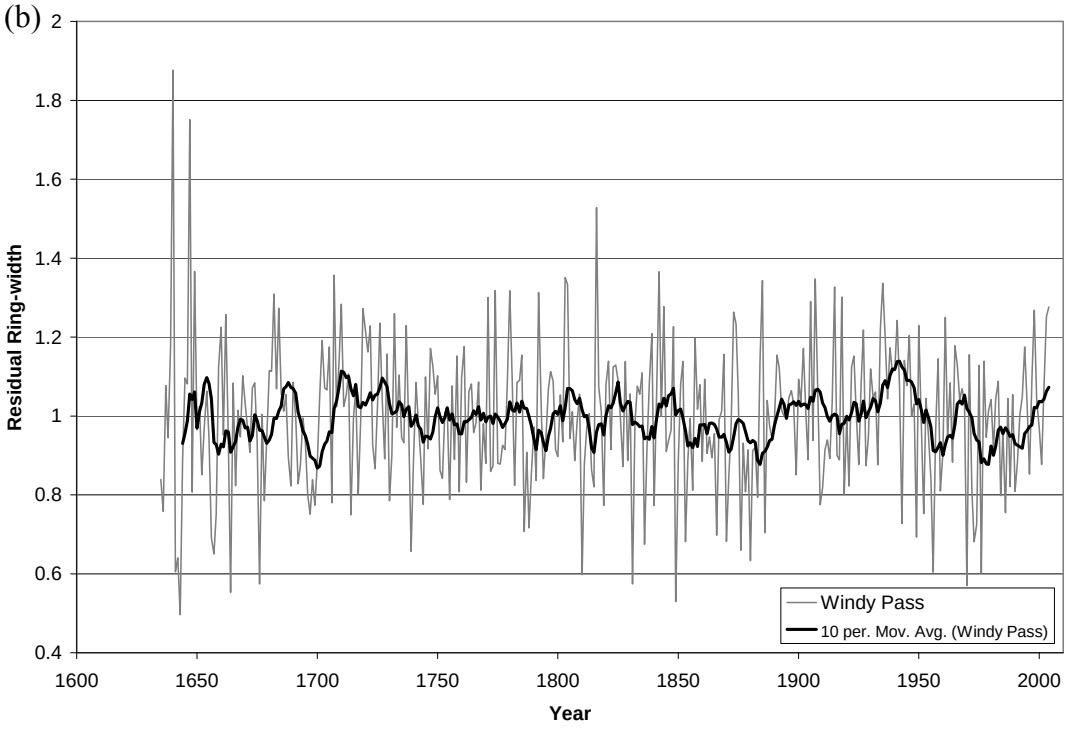
Residual Ring-width
2
1.8
1.6
1.4
1.2
1
0.8
0.6
0.4
1600
1650
1700
1750
1800
1850
1900
1950
2000
Year
Windy Pass
10 per. Mov. Avg. (Windy Pass)

(c)

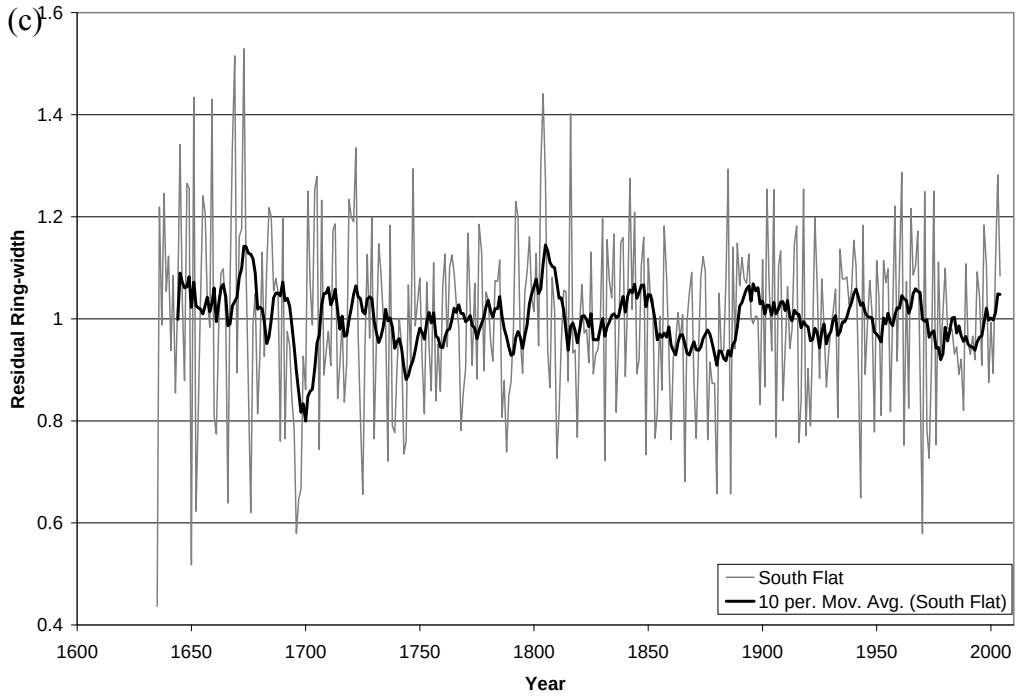
Residual Ring-width
1.6
1.4
1.2
1
0.8
0.6
0.4
1600
1650
1700
1750
1800
1850
1900
1950
2000
Year
South Flat
10 per. Mov. Avg. (South Flat)

correlated (r = 0.568), the White and Surprise sites are only slightly less correlated (r = 0.539; Table 2.2). Given the strong similarities between the chronologies, they were combined to form a regional master chronology with 87 cross dated series spanning 412 years (1596 to 2007; Figure 2.5). Five individual series did not significantly cross date and were removed. The EPS cutoff is at 1680, leaving the regional chronology with a mean inter-series correlation of 0.544 and an average mean sensitivity of 0.244.

Table 2.2: Correlation matrix showing interseries correlations between site chronologies and master chronology.

	Surprise	Windy Pass	South Flat
Surprise	-	0.560	0.539
Windy Pass	0.560	-	0.568
South Flat	0.539	0.568	-

2.5.2 Climate station analysis

The Stewart Airport and Dease Lake stations experience significantly different climates. At Stewart Airport the mean annual temperature is 5.6°C (± 3.5°C); whereas Dease Lake it averages -0.9°C (± 4.1°C; Figure 2.6). Average summer growing season air temperatures in June-July-August (JJA) are considerably different between the two stations, with conditions warmer at Stewart (mean JJA 14.3°C) than at Dease Lake (mean JJA 11.7°C).

Figure 2.5: Living mountain hemlock chronology displayed with a five-year running mean. The number of series included in the chronology (sample depth) is shown at the bottom of the graph. The master chronology contains 27 series; the series intercorrelation value is 0.544 and the average mean sensitivity is 0.244.

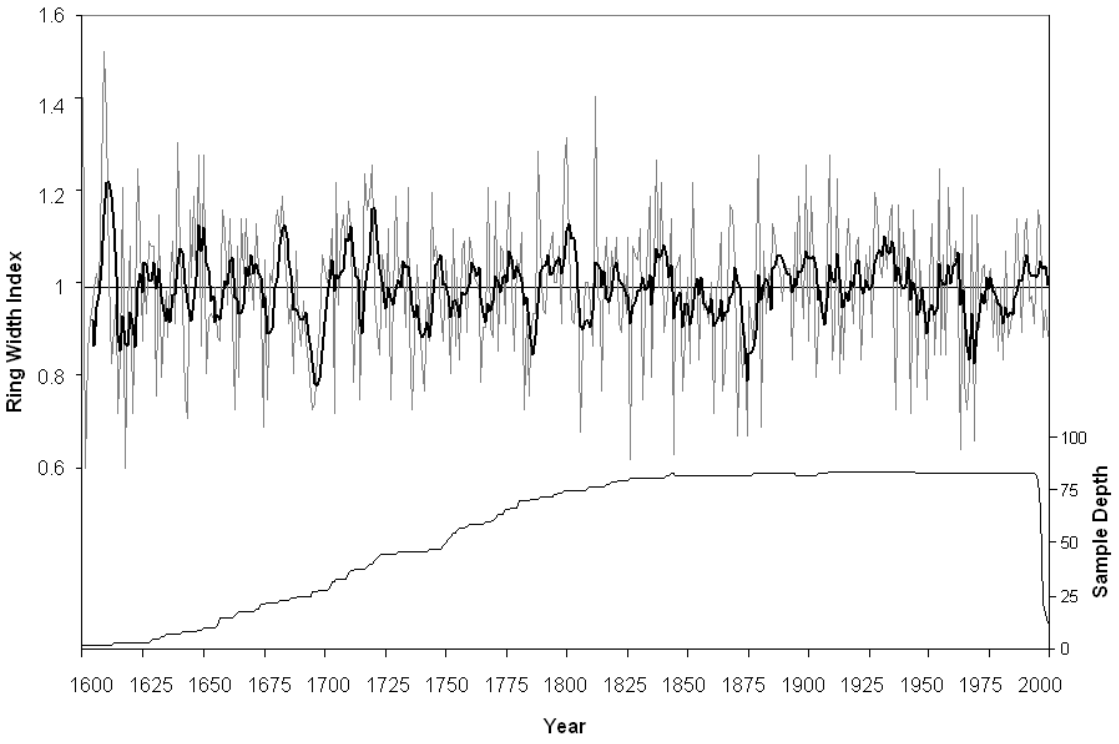

Figure 2.6: A comparison of annual mean air temperature between Stewart Airport and Dease Lake.

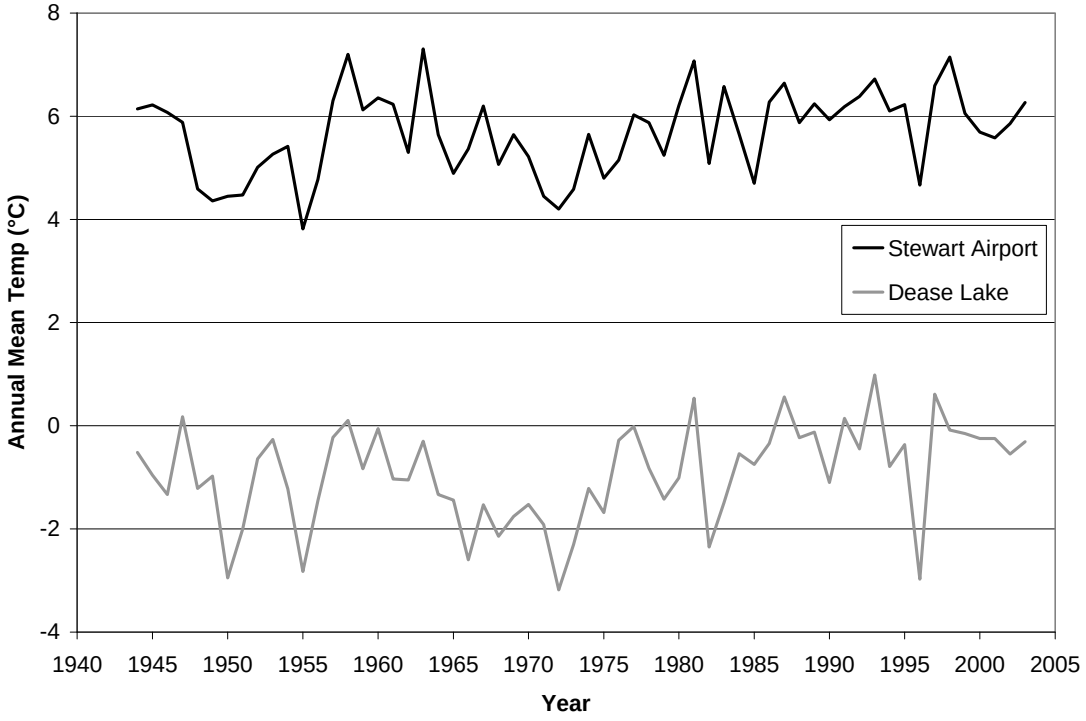

Overall trends in the JJA air temperature show a 0.2°C warming in both instrumental data sets over the period of record (Figure 2.7). When analysing the overall trends, however, periods of warming and cooling are seen. At Stewart Airport, air temperatures warmed by 1°C from 1952 to 1978, followed by cooling of around 0.9°C from 1979 to 2001. The trend at Dease Lake is the opposite, with a -0.9°C cooling from 1958 to 1978, and 1.8°C of warming from 1979 to 2001.

Figure 2.7 compares the annual mean precipitation at Stewart Airport and Dease Lake. At Stewart Airport total annual precipitation increased by 210 mm between 1910 and 2005. At Dease Lake, total annual precipitation increased by 25 mm between 1946 and 2003.

Figure 2.7: A comparison of annual mean air temperature between Stewart Airport and Dease Lake.

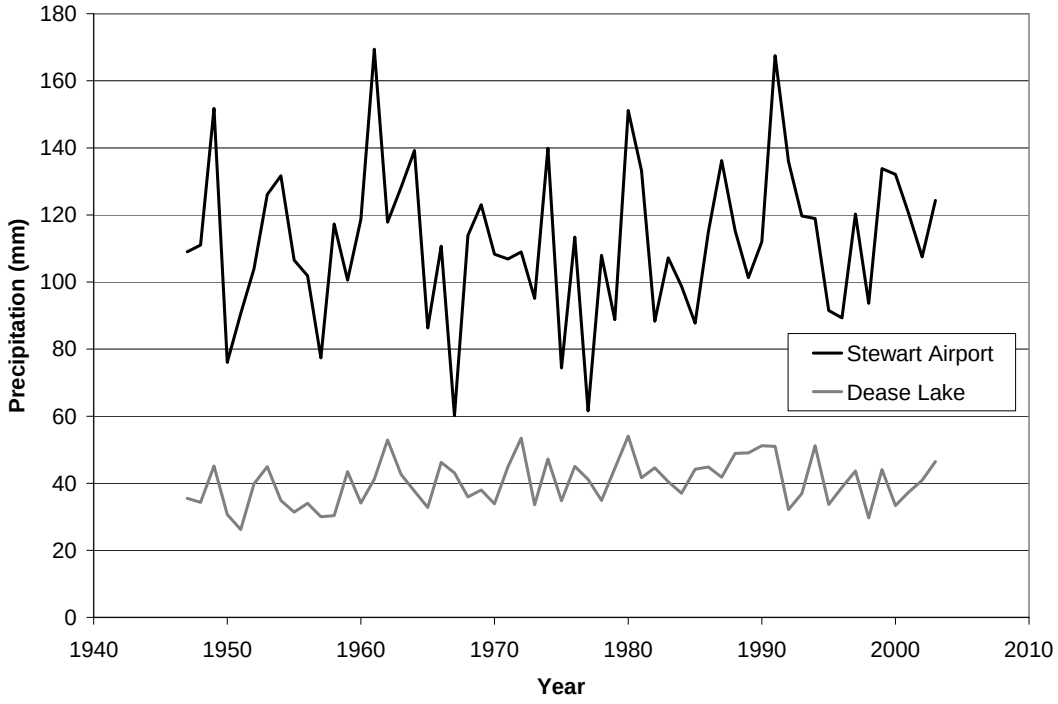

2.6 Analysis

2.6.1 Climate-Growth Responses

The master tree-ring chronology was compared to mean monthly precipitation and monthly records of mean, minimum, and maximum temperature from both the Stewart and Dease Lake stations using DENDROCLIM2002. Correlations between ring width and climate variables from Stewart Airport and monthly precipitation totals at Dease Lake were all insignificant (Table 2.3). The chronology did, however, exhibit a strong positive correlation to the average mean JJA air temperature at Stewart (Figure 2.8) ($r = 0.48$ for the ring width chronology) and Dease Lake ($r = 0.58$ for the ring-width chronology).

Table 2.3: Correlations between instrumental climate variables and the residual regional chronology. Significance level = 0.01.

Variable	Stewart Airport[1]	Dease Lake
Minimum July Temperature	0.24	0.37
Maximum July Temperature	0.26	0.36
Mean July Temperature	0.14	0.49
Mean June-July-August Temperature	0.48	0.58
Total Monthly Precipitation	0.11	0.24

Figure 2.8: Coefficients calculated between the mountain hemlock chronology and the mean temperature time series from Dease Lake using DENDROCLIM2002. The black bars represent correlation coefficients; the gray bars represent response function coefficients. Months in block letters are from the previous year.

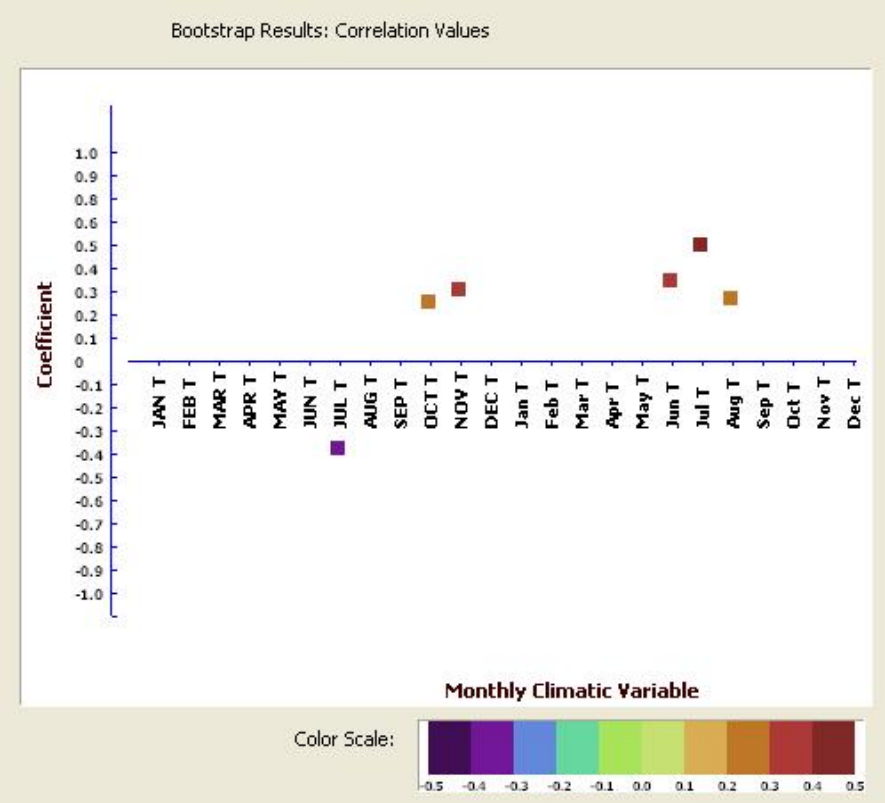

The climate-radial growth scatterplot suggests a linear relationship exists between tree-ring growth and mean JJA air temperature at Dease Lake ($r^2 = 0.34$; Figure 2.9). An evolutionary moving average analysis (48 year blocks) performed with DENDROCLIM2002 indicates this relationship is consistent through time (Figure 2.10).

Figure 2.9: Scatterplot comparing the radial growth of mountain hemlock and average June-July-August temperature at Dease Lake over the instrumental record (1943 – 2003).

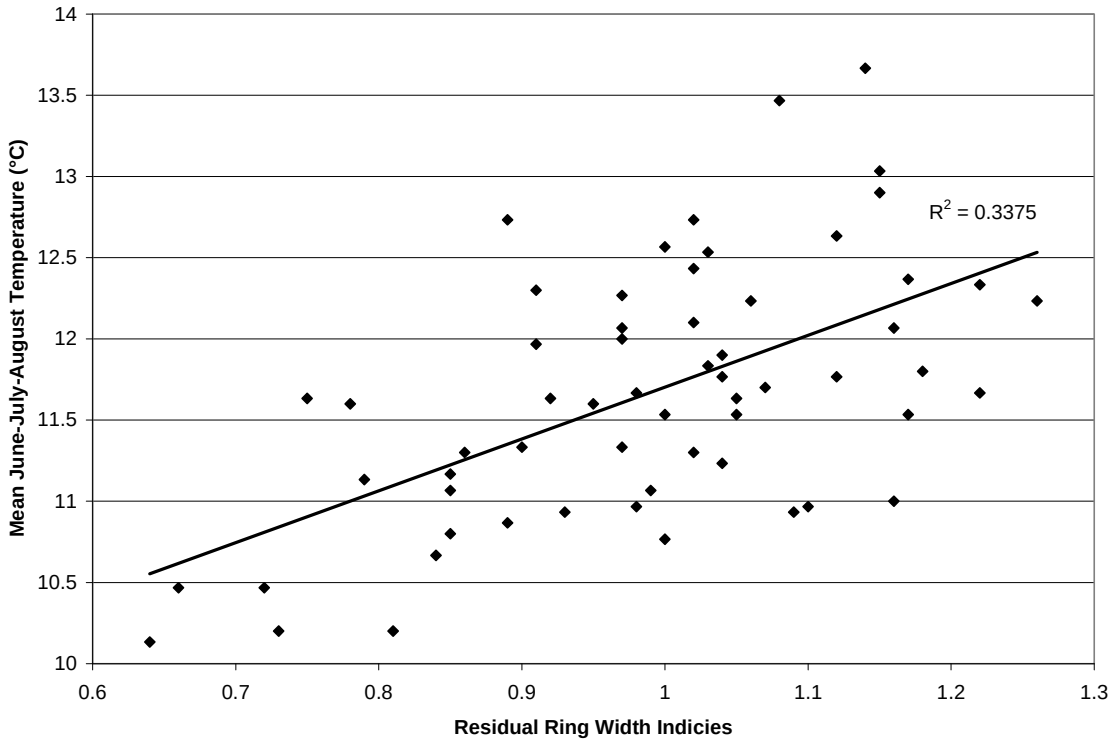

This climate-radial growth relationship is consistent with previous studies (Smith and Laroque 1998; Gedalof and Smith 2001a). It suggests that warm air temperatures in the JJA growing season lead to increased radial growth in mountain hemlock trees in this region (Figure 2.9).

Figure 2.10: This figure illustrates bootstrapped moving interval response function analyses calculated using the program DENDROCLIM2002. Forty-eight year intervals were employed to test the strength of relationships between tree ring indices and the Dease Lake monthly June to August air temperature values over time. The panels depict the relationships between the mountain hemlock chronology and mean temperature values. Statistically significant positive relationships are highlighted in shades of red and negative relationships in shades of blue. Months of the previous year are identified with capital letters.

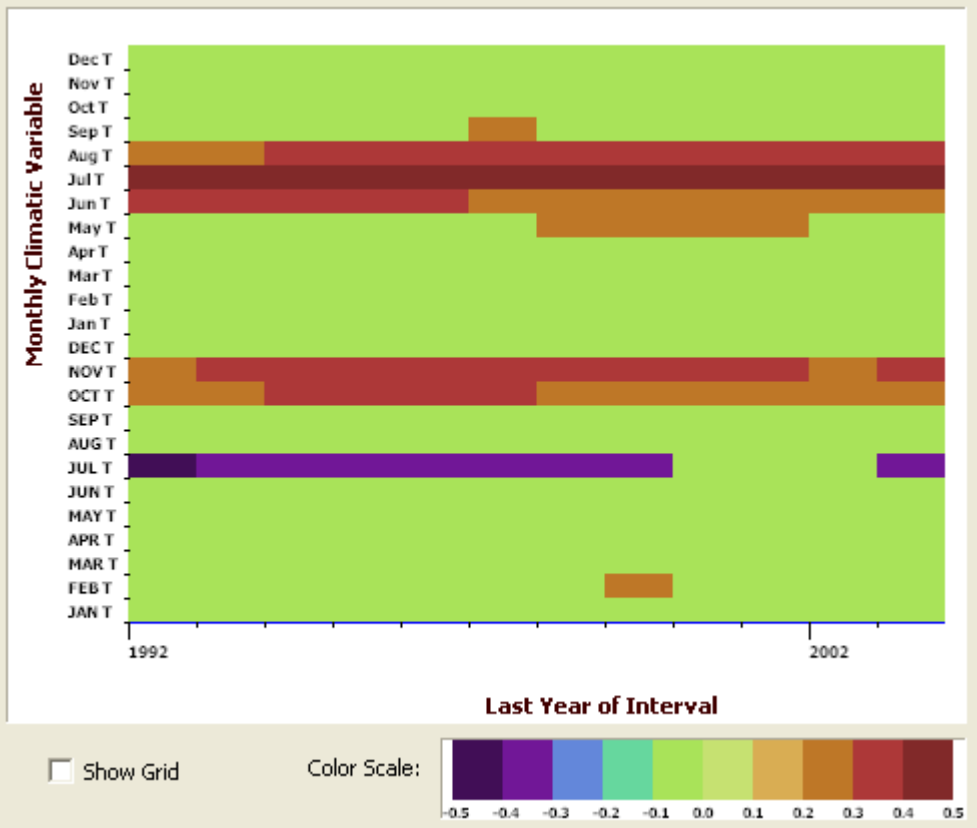

2.6.2 Dendroclimate Reconstruction

Linear regression was used to model the relationship between mean JJA air temperature and radial growth for the period from 1944 to 2003, with split-verification partitioning the data into a 28 year calibration period from 1974 to 2003 and a 30 year verification period from 1944 to 1974 (Fritts 1976). The

modeled temperatures significantly correlate with the instrumental data (r = 0.63; Table 2.4), with the model successfully tracking low-frequency variations in both the calibration and the verification periods (Figure 2.11). Given the strength of the modelled relationship, a proxy record of mean JJA air temperature was constructed extending to 1680 (Figure 2.12). Over the period of record the coolest summers occurred in 1706, 1810, 1880, 1970 and 1976. The warmest summers occurred in 1792, 1804, 1816, 1885 and 1915.

Figure 2.11: June-July-August temperature model based on a linear relationship with the radial growth of mountain hemlock.

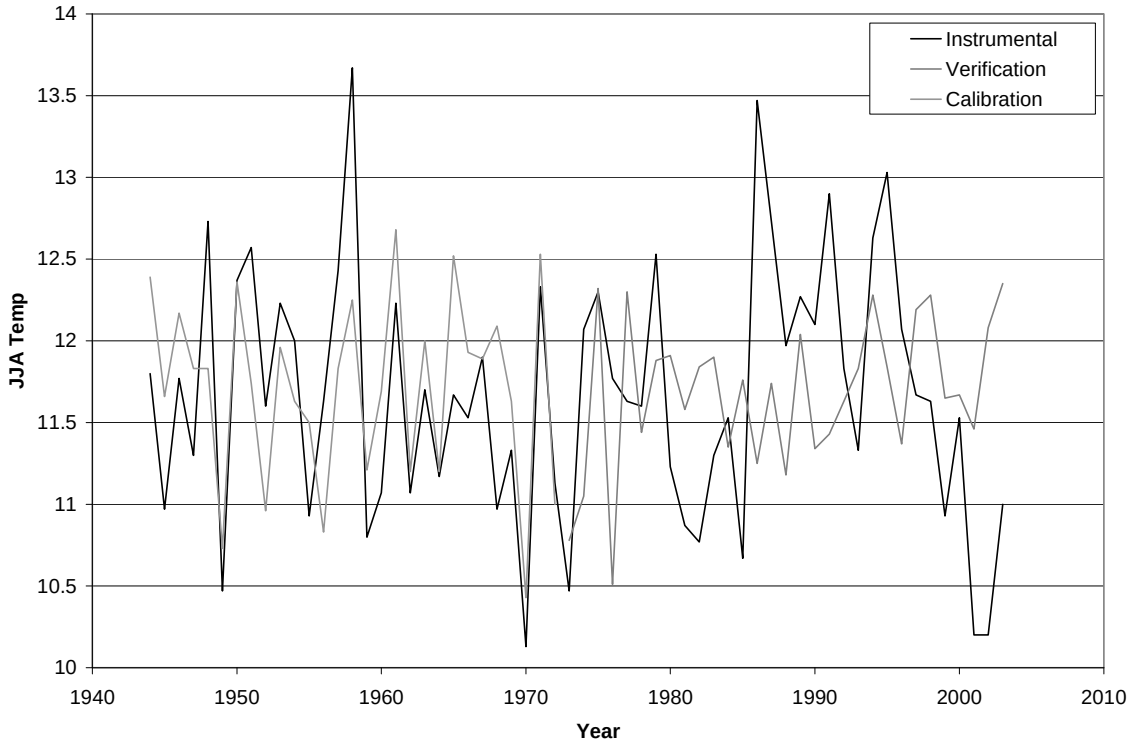

Figure 2.12: Reconstructed precipitation anomaly record for the Cambria Icefield. The thick black line represents a 10 year running mean.

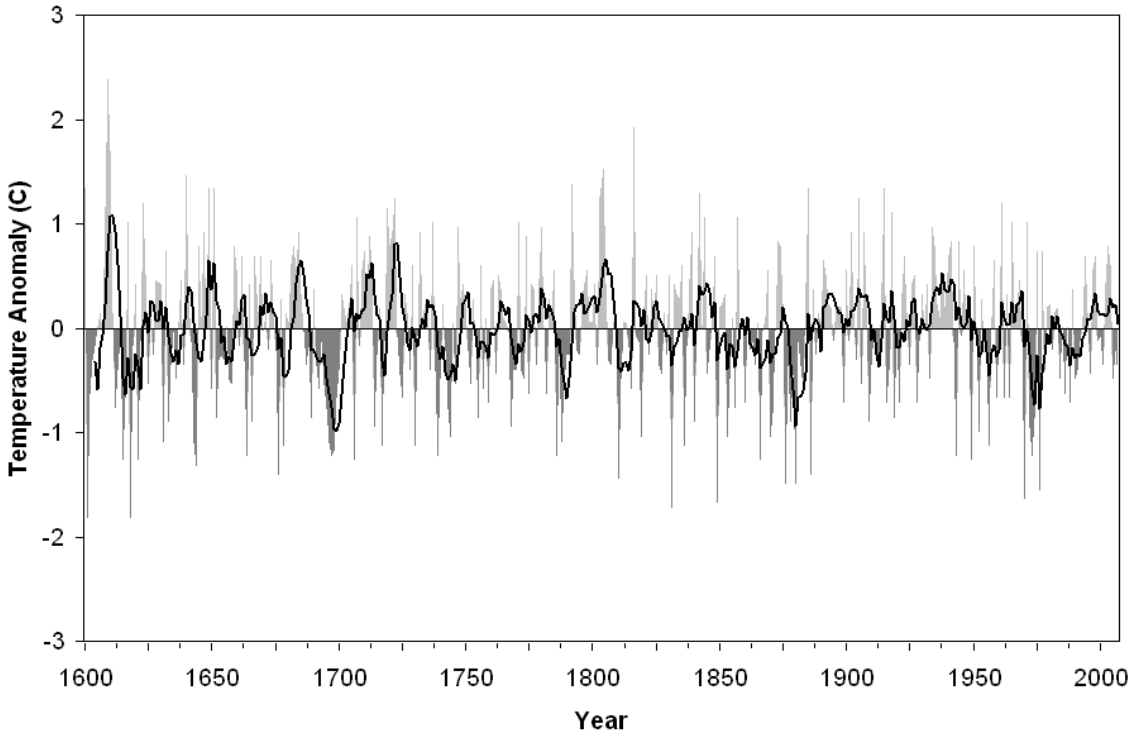

2.6.3 PDO and ENSO Circulation Patterns

The master tree-ring chronology correlates with SST in the Northeast Pacific and South Pacific oceans from 1870 to 2007 (Figure 2.13). Positive correlations (r = 0.3) occur across an east-west equatorial belt centred at 170° east and terminating off the northwest coast of South America. These spatial relationships are interpreted as reflecting a radial growth response to warmer-than-normal temperatures during positive ENSO phases.

A positive relationship (r = 0.4) exist between radial growth and SST between 42° to 63° N offshore of PNA. The persistence and strength of these correlations suggest that a causal relationship exists between

Figure 2.13: Tree ring index – June-July-August sea surface temperature correlation. The tree rings have a positive relationship (r = 0.2 to 0.3) to sea surface temperatures across the equator, along the South American coast to 30˚ south, and off the coast of northern BC and Alaska. There is a negative correlation (r = -0.2 to -0.4) with sea surface temperature in the central north Pacific.

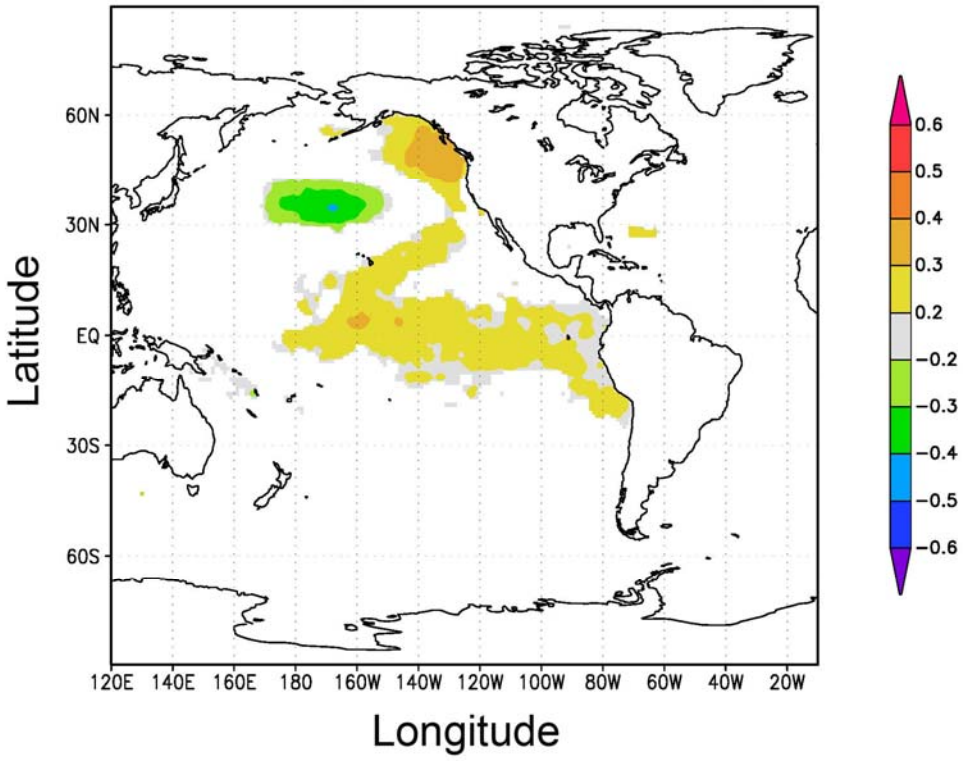

radial growth and positive PDO phases that bring above normal summer growing season temperatures to this region (Mantua *et al.* 1997).

The wavelet analysis aims to decompose a time series into time and space simultaneously and highlights both low and high frequency variability within the reconstructed proxy temperature record (Torrence and Compo 1998). Figure 2.14 indicates frequent 8-year period events (marked in red) from 1600-1700-1820, 1870-1900 and 1960-1980, typical of ENSO, and weaker (shown in yellow) 32-year period events from 1680-1720, consistent with the significant variance of PDO

behaviour (Mantua and Hare 2002). A weakening of the PDO influence from 1800 and 1900 matches PDO reconstructions over this time period (Gedalof and Smith 2001b).

Figure 2.14: (a) Summer Temperature Anomalies. (b) The wavelet power spectrum. The contour levels are chosen so that 75%, 50%, 25%, and 5% of the wavelet power is above each level, respectively. Black contour is the 5% significance level, using a white-noise background spectrum. (c) The global wavelet power spectrum (black line). The dashed line is the significance for the global wavelet spectrum, assuming the same significance level and background spectrum as in (b).

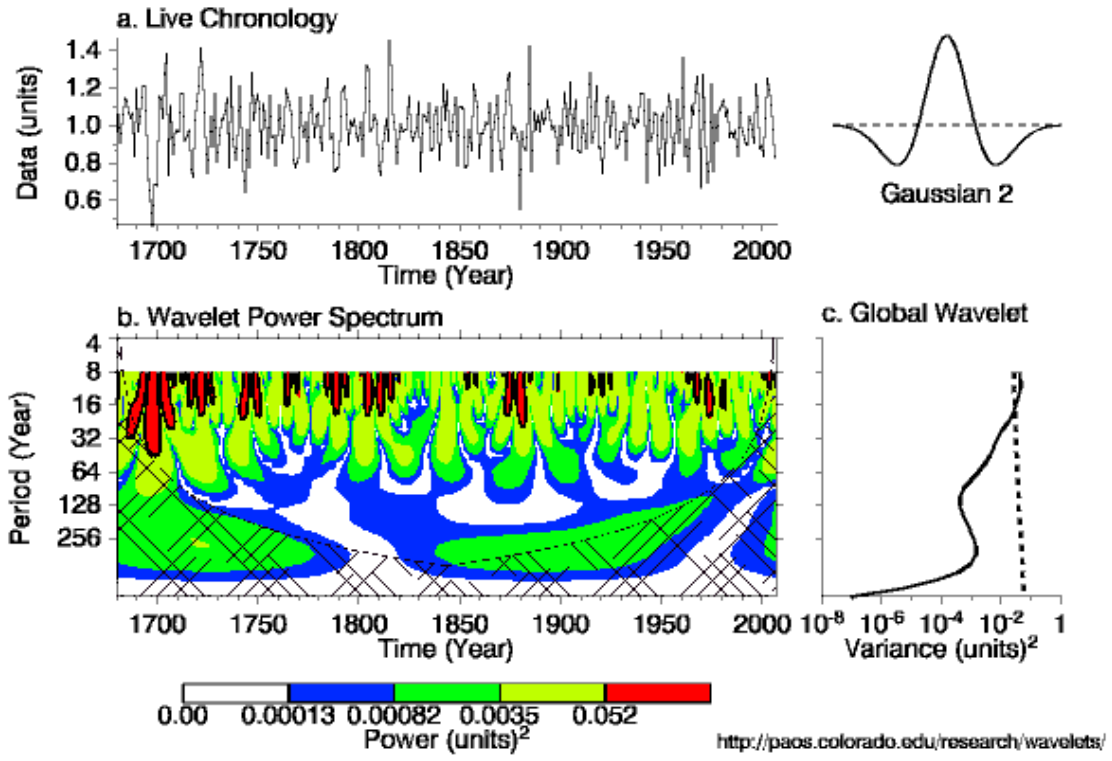

2.7 Discussion

The radial growth of mountain hemlock trees along the eastern slopes of the northern Coast Mountains appears to be influenced by mean JJA air temperature. This climate-radial growth relationship is assumed to reflect either a physiological response to increased rates of photosynthesis during warm summers (i.e., Kramer and Kozlowski 1960) or, alternatively, an indirect response resulting from accelerated melting of the seasonal snowpack during warm summers. The outcome is an extension of the growing season and potentially an extension of the period over which cambium is produced.

These findings are largely consistent with those of earlier dendroclimatological investigations in PNA (Smith and Laroque 1998; Gedalof and Smith 2001a). However, most previous research has highlighted a negative relationship between the radial growth of mountain hemlock trees and spring snowpack depth (Graumlich and Brubacker 1986; Peterson and Peterson 2001; Smith and Laroque 1998); as well as a positive relationship with summer precipitation (Brubaker 1990). The reduced importance of seasonal precipitation in this setting is noteworthy and is attributed to rainshadow effects that lead to relatively dry leeward slopes (Environment Canada 2009).

The three forest stands sampled in this study are found close to the easternmost extent of mountain hemlocks in the region where they are almost certainly periodically impacted by cold continental temperatures (Means 1990). It is also possible that in this setting the physiological role played by the seasonal

snowpack is not as significant as in more maritime settings (Smith and Laroque 1998; Larocque and Smith 2005). If this is the case, it is hypothesized that cool summer temperatures significantly limit the radial growth of mountain hemlocks.

The mean JJA proxy air temperature record constructed in this study illustrates warmer and cooler periods that are synchronous with those developed using dendroclimatological methodologies at other locations in the central and northern Coast Mountains (i.e., Gedalof 2002; Larocque and Smith 2003). Across this region cooler than normal JJA air temperatures characterize the intervals between 1698 to 1706, 1876 to 1886, and 1970 to 1976 (Figure 2.12). Warmer than normal JJA air temperatures occurred from 1715 to 1726, 1800 to 1820, 1900 to 1920 and 1945 to 1955. These alternating warm-cold temperature regimes are in step with phases changes in the PDO and highlight the effect of both 'warm' and 'cold' PDO phases changes on JJA air temperature in this region.

Like many previous dendroclimatological reconstructions this proxy record fails to accurately model extreme values (Figure 2.12). As only a moderate percentage of growth in any given year can be attributed to a single climate variable (Fritts 1976), the model response may be attributed to the role other limiting factors to growth play in anonymously warm or cool summers (i.e., Ettl and Peterson 1995). Given that variations in summer precipitation and spring snowpack depth have been shown to impact the radial growth of mountain hemlocks in many regions of PNA, it may be that during certain years the direct role of temperature diminishes.

Glacial histories from the northern Coast Mountains suggest their behaviour reflects a shared mass balance response to the temperature trends recorded in the proxy reconstruction. Jackson *et al.* (2008) show that glaciers were advancing in the Todd Icefield area from 1746 to 1764 and from 1843 to 1899. These intervals coincide with periods of lower than average summer temperature (Figure 2.12), suggesting that positive mass balances may be attributed to colder summer climates at this time.

Recent research has led to recognition that trees located in climatically-sensitive at high altitude and latitude sites sometimes display an inconsistent radial growth response to climate through time (Visser *et al*. 2010). This divergent behavior appears confined to recent decades and hence strongly suggests an anthropogenic cause (Cook *et al.* 2004). In this instance, however, a bootstrapped moving interval response function analysis shows that over the period of instrumental record, mountain hemlock radial growth has consistently positively responded to JJA air temperatures (Figure 2.10). This finding suggests that as the Stewart region receives large amounts of winter precipitation, two responses occur: the ground is insulated during the winter months and hence soil water content is not a limiting factor and warm spring air temperatures in the spring melt the snowpack. Hence shallower snowpacks melt earlier in the season, and therefore tree-ring growth can occur over a longer period of time.

2.8 Summary

A 400-year long mountain hemlock tree-ring chronology was constructed from increment samples collected at three sites in the northern Coast Mountains. Response function analysis showed that over the period from 1946 to 2007, the annual increment of radial growth was correlated to mean June-July-August temperature. A linear model was constructed to represent this relationship over the duration of the well-represented portion of the chronology.

The proxy temperature anomaly record constructed as part of this study extends from 1680 to 2007. Represented within the reconstructed record of summer temperature were extended intervals of warmer and cooler periods that closely match those previously reconstructed. Analysis of the likely casual factors responsible for these long-term variations in temperature showed that climate forcing events described by the PDO and ENSO indices have played a significant role in long-term climate changes in this region.

In summary, this study demonstrates how temperature-sensitive trees can be used to reconstruct robust proxy climate records for remote settings in northwestern British Columbia. Notably, the reconstruction expands upon the large-scale temperature reconstructions presented by Briffa *et al*. (1994) and Briffa *et al.* (2001), by providing a detailed regional reconstruction of treeline temperature anomalies over the last 300 years. Understanding of the causes and effects of climate changes in this setting is crucial for evaluating the linked long-term hydroclimatic and glaciological impacts.

Chapter 3

Dendroglaciological reconstruction of late Holocene glacier activity at White and South Flat Glaciers, Boundary Range, northern British Columbia Coast Mountains

3.1 Introduction

The rapid retreat and downwasting of glaciers in Pacific North America (PNA) over the last few decades is exposing land surfaces and glacially-killed trees that provide singular insights into periods of glacier activity during the Holocene epoch. Recent and ongoing investigations in this region show that glaciers repeatedly advanced and retreated over the last eight millennia (Calkin *et al.* 2001; Menounos *et al.* 2009; Wiles *et al.* 2008). These discoveries are challenging earlier findings that Holocene glacier expansion was largely restricted to the Neoglacial period (Denton and Stuiver 1966; Ryder and Thompson 1986).

Recognition of the dynamic character of glacier activity in the Holocene suggests a greater number of climate shifts than is recorded in many paleorecords from the region (Walker and Pellatt 2003). To understand the frequency and significance of these shifts, high resolution, long-term temporally significant records are required. Annually-resolved tree-ring records from living trees and subfossil samples provide an opportunity to place current glaciological changes into a longer term climatological context (Swetnam and Betancourt 1997).

Our understanding of Holocene glacial history in the mountains of PNA is incomplete. There are regions where little or no research focused on this topic has

been completed (Menounos *et al.* 2009). In British Columbia (B.C.), one such location is the northern Coast Mountains where limited research indicates that dendroglaciological records spanning the Holocene are present (i.e., Ryder 1987; Clague and Matthewes 1996; Jackson *et al.* 2008). The goal of the research presented in this chapter was to describe the late Holocene history of two glaciers flowing from the Cambria Icefield (Figure 3.1). Reconnaissance investigations in July 2008 revealed fresh exposures of subfossil wood buried in and below glacial sedimentary units. Additional sites and detrital subfossil wood deposits were discovered during a return expedition to the site in July 2009. Dendroglaciological research methodologies were applied to describe the ice front behavior of these two glaciers and to consider the climatological context of their Holocene behaviour.

3.2 Research Background

3.2.1 Tree-rings and dendroglaciology

Dendrochronological techniques can be applied to study and date the movement of glaciers (Luckman 1998; Smith and Lewis 2007a). Dendrochronology, or the study of tree-rings, deals with the dating and study of annual growth rings (Fritts 1976). As the radial growth of trees in the midlatitudes is largely limited by annual variations in climate, tree-ring records can be cross dated to provide chronological and temporally extensive paleoenvironmental records (Fritts 1976).

Dendroglaciological methodologies use tree-ring evidence to provide insights into prehistorical glacier activity in two ways. Living-trees found growing

Figure 3.1: Location of the Cambria Icefield and key glaciers within the vicinity and referred to in the text.

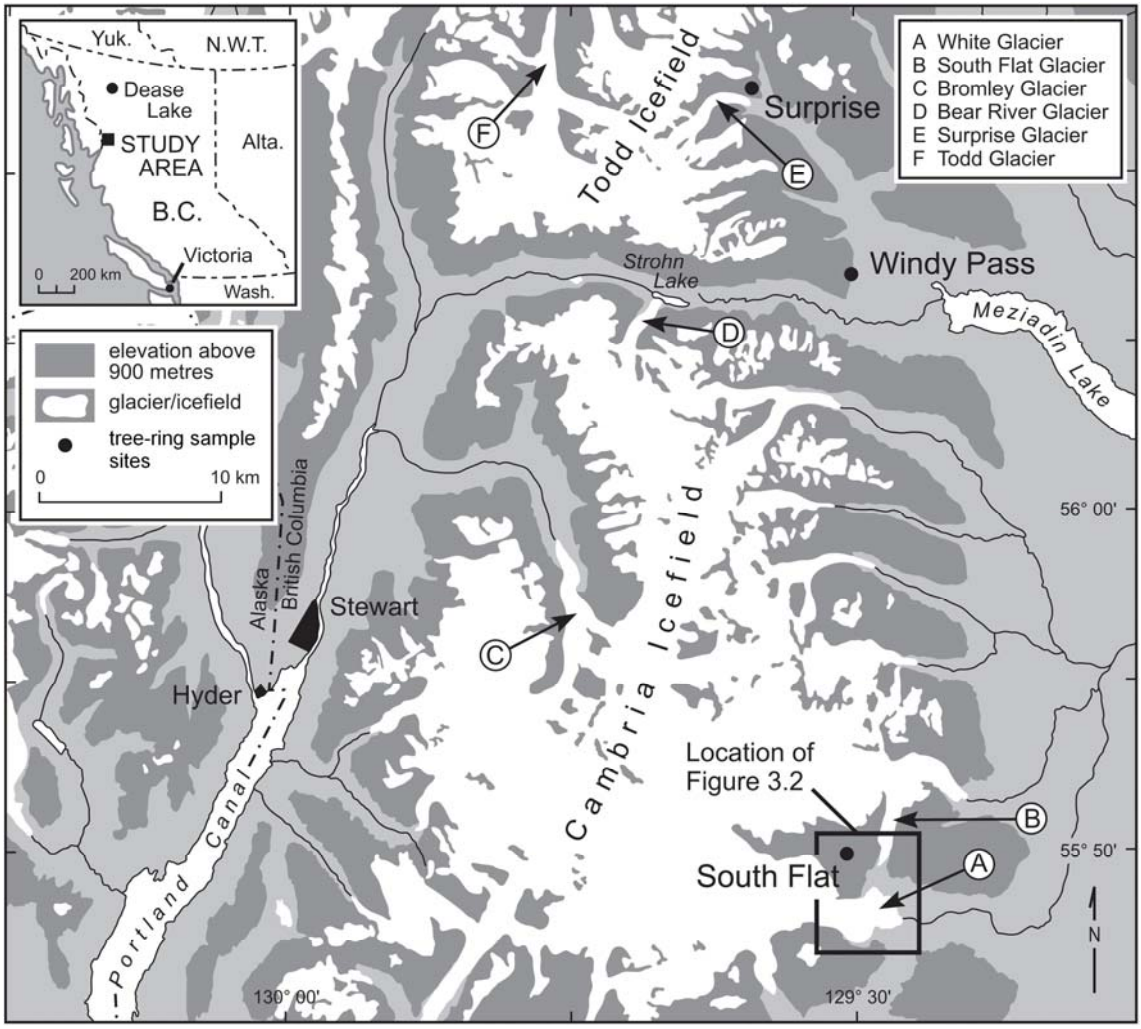

on recently deposited glacier deposits and landforms, or that were scarred by glacier activity, can be absolutely dated to provide minimum ages of surface stability and ice movement (Luckman 1998). In the case of moraines, the age of the oldest tree found growing on the deposit highlights the point in time when a glacier began to downwaste and/or retreat in response to a negative mass balance shift (Watson and Luckman 2004). Detrital wood and *in situ* tree stumps buried within or below glacial sedimentary units provide insights into intervals of glacier expansion and retreat (Smith and Lewis 2007b). The kill dates of subfossil wood samples are established by cross dating to dated tree-ring chronologies or are referenced to radiocarbon-dated floating tree-ring chronologies to provide relative insights into when they were overwhelmed by an advancing glacier.

3.2.2 Holocene Glacial Activity in the British Columbia Coast Mountains

The Coast Mountains flank the Pacific Ocean in western Canada, extending for 1,500 km along the B.C. coastline (Ryder and Thomson 1986). This rugged high relief mountainous terrain is characterized by glacier landforms and deposits that reflect extended episodes of Pleistocene glaciation (Clague and James 2002).

During the late Wisconsinan glaciation the Cordilleran ice sheet mantled the Coast Mountains, reaching its maximum size and extent around 16,500 ^{14}C years BP (Clague 1989). Ice began to downwaste by 13,000 ^{14}C years BP and by the beginning of the Holocene glaciers had retreated to positions similar to those reached at the present time (Fulton 1984; Clague 1989).

Seven periods of Holocene glacier expansion are recognized in B.C.: at ca. 8000 ^{14}C years BP (Menounos *et al*. 2009); between 6,000 to 5,000 ^{14}C years BP (Ryder and Thompson 1986); at ca. 4200 ^{14}C years BP (Koch *et al.* 2007, Osborn *et al.* 2007); at ca. 3000 ^{14}C years BP (Ryder and Thomson 1986); at ca. 2300 ^{14}C years BP (Jackson *et al.* 2008; Smith and Koehler 2010); at ca. 1700 to 1500 ^{14}C years BP (Reyes *et al.* 2006); and, during the Little Ice Age (LIA) in the Coast Mountains which began as early as 1000 A.D. and ended as late as the 20th Century (Desloges and Ryder 1990; Larocque and Smith 2003; Allen and Smith 2007).

Glacier expansion between 1700 and 1500 ^{14}C years BP is referred to as the First Millennium Advance (FMA) and is expressed throughout PNA (Reyes *et al.* 2006). During this episode, glaciers advanced down valley to positions slightly less extensive than their LIA positions (Ryder and Thomson 1986). The FMA appears to incorporate two phases of glacier advance and retreat separated by an interval of reduced glacier size (Jackson *et al.* 2008; Barclay *et al.* 2009).

Evidence for glacier activity during the LIA is widespread in the Coast Mountains where early and late phases of expansion are recorded (Larocque and Smith 2003). Evidence for ice expansion following retreat of FMA ice fronts comes from Lillooet and Bridge glaciers in the southern Coast Mountains (Reyes and Clague 2004; Allen and Smith 2007) and in the northern Coast Mountains at Bear Glacier (Haspel *et al.* 2005; Spooner *et al.* 2005). The spatial extent of this evidence throughout the Coast Mountains suggests that glaciers were likely expanding down valley by 1000 A.D.

Maximum ice front extents in the early-LIA were reached in the 1300s to 1400s at many sites, followed by an interval of ice retreat that ended by the late-16th Century when glaciers were again advancing down valley (Larocque and Smith 2003). Many glaciers in the region are fronted by terminal moraines dating to an early 18th Century advance, with a subsequent readvance in the 19th Century recorded by the construction of moraines commonly located immediately up valley (Smith and Desloges 2000; Larocque and Smith 2003; Koch *et al.* 2007).

3.3 Research Area

The Cambria Icefield is situated 35 km southeast of Stewart, B.C. (Lat 55° 47' N, Long 129° 29' W; Figure 3.1). Located within the Boundary Ranges, the icefield covers an area of 715 km^2 and includes within its boundaries Treble Mountain whose summit reaches 1830 m asl. Large outlet glaciers spill into surrounding valleys to present-day terminus positions located between 885 to 510 m asl.

The icefield area is underlain by Jurassic Hazelton Group volcanics consisting of siltstone, greywacke and sandstone bedrock (Grove 1973). High elevation montane forests are characterized by mixed stands of mountain hemlock (*Tsuga mertensiana* [Bong.] Carr.) and subalpine fir (*Abies lasiocarpa* [Hook.] Nutt.; Meidinger and Pojar 1991). The upper treeline is found at around 1500 m asl.

The Holocene behaviour of glaciers in the region is only poorly documented. Ryder (1987) described evidence for LIA advances in the Stikine-Iskut area to the north that culminated during the early or middle part of the 18th Century, followed

by a second advance that ended during the late 19th to early 20th Century. Clague and Mathews (1992) and Clague and Mathewes (1996) examined proglacial lake and fen sediments peripheral to the Berendon Glacier describing evidence for an expansion of glacier ice at ca. 3000 ^{14}C years BP, during the FMA and the LIA. Glaciers originating from the Todd Icefield 35 km north of the Cambria Icefield expanded down valley prior to 3000 ^{14}C years BP, at 3000 ^{14}C years BP; and at 2300 ^{14}C years BP (Jackson *et al.* 2008). Distinct intervals of FMA expansion were recorded at 1700 and 1450 ^{14}C years BP. Three episodes of LIA expansion occurred at 750 ^{14}C years BP (1250 A.D.), 240 ^{14}C years BP (1750 A.D.) and 100 ^{14}C years BP (1900 A.D.).

Little is known of the Holocene behaviour of the Cambria Icefield and its glaciers. At the Bear River Glacier (Figure 3.2), where ice cascades down to Bear Pass from the north end of the Cambria Icefield, Haspel *et al.* (2005), Spooner *et al.* (2005) and Jackson *et al.* (2008) dated wood mats buried within lateral moraine sediments that record three intervals of ice expansion from 3700 to 3300 ^{14}C years BP. Haspel *et al.* (2005) and Spooner *et al.* (2005) describe a subsequent period of significant ice accumulation in the early LIA at 1040 ^{14}C BP.

Over the historical period glaciers in the Cambria Icefield area have down-wasted and receded 2.5 to 6 km upvalley from LIA terminal positions located from 815 to 380 m asl. McConnell (1913) recorded 50 m of retreat at the north-facing Bromley Glacier from 1910 to 1911, and observed that it been in recession for some time. Following this observation Field (1969) noted that the Bromley Glacier continued to retreat 30 m/yr up valley from 1911 to 1946. Mathews (1965)

Figure 3.2: Site map of the White Glacier and South Flat valley, showing the location of the glaciers and study sites.

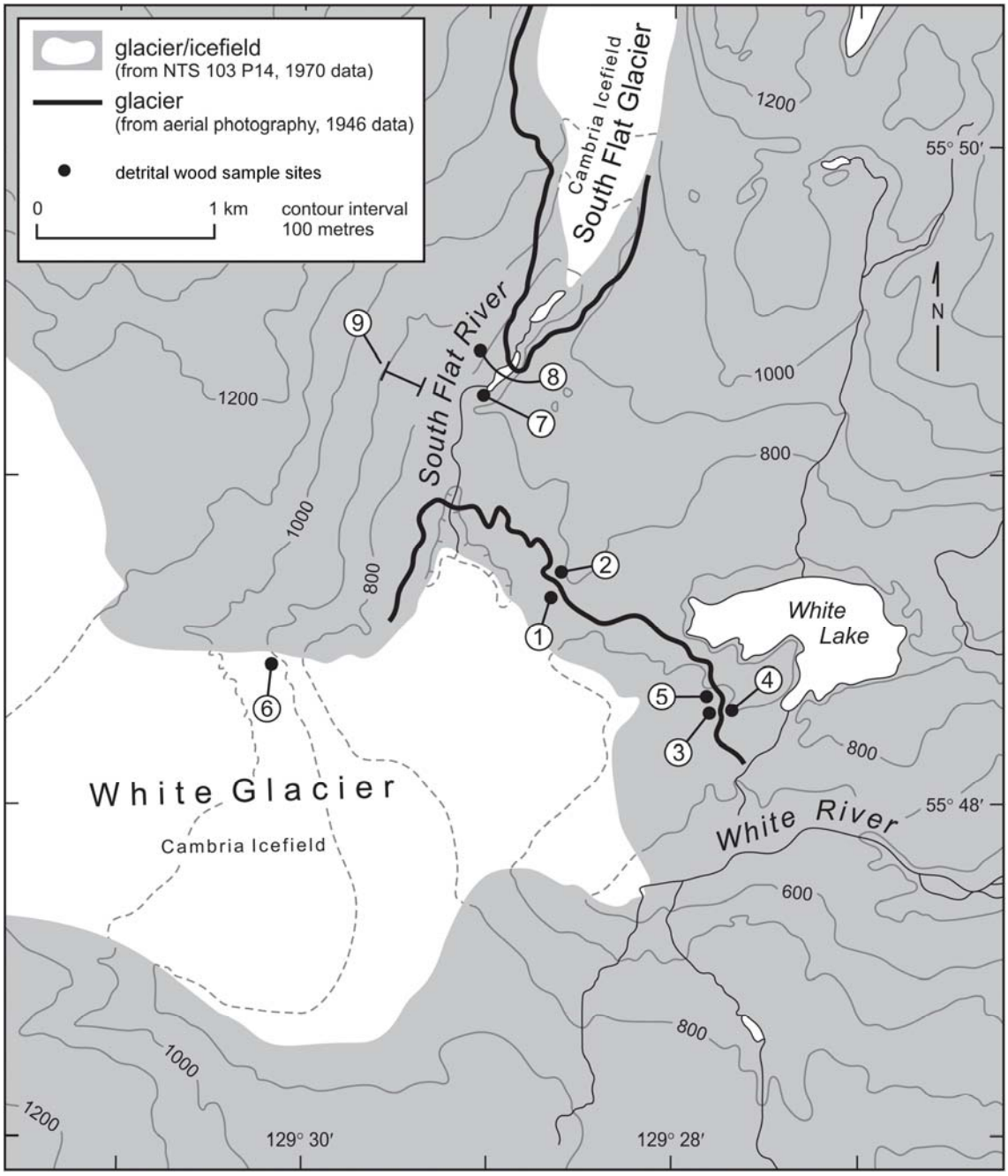

reports that retreat of Bear River Glacier in the 1940s and 1950s led to the impoundment of ice-proximal Strohn Lake. In the adjacent Todd Icefield area, Jackson *et al.* (2008) recorded terminus retreat rates at five glaciers at rates varying from 9 to 76 m/yr between 1974 and 1997.

3.3.1 Study Sites

Field investigations were undertaken in the adjacent and recently deglaciated forefields of White and South Flat glaciers (*unofficial names*, Figure 3.2). The glaciers were confluent during the LIA but separated prior to the earliest known photograph from 1946 (Table 3.1). A prominent ridge and trimline associated with White Glacier demarcates its' maximum upvalley expansion into the adjacent South Flat valley (Figure 3.3).

Table 3.1: Estimated historical terminus retreat rates at the White Glacier and the South Flat Glacier.

Glacier	Date	Aerial Photograph Number	Total Retreat (m)	Retreat Rate (m/year)
White	2001	15BCB01007	255	51
	1996	30BCC96058	113	10.3
	1985	30BC85047	417	10.7
	1946	A12276		
South Flat	2001	15BCB01007	149	29.8
	1996	30BCC96058	170	15.5
	1985	30BC85047	312	6.3
	1946	A12276		

White Glacier (Lat 55° 51'N, Long 129° 31'W; Figure 3.2) flows eastward from the Cambria Icefield and presently terminates at 820 m asl adjacent to South Flat River, a tributary to White River. The LIA extent of White Glacier is

Figure 3.3: Aerial photograph from 1991. The white line demarcates White and South Flat glaciers' maximum upvalley extent during the LIA (see Figure 3.21).

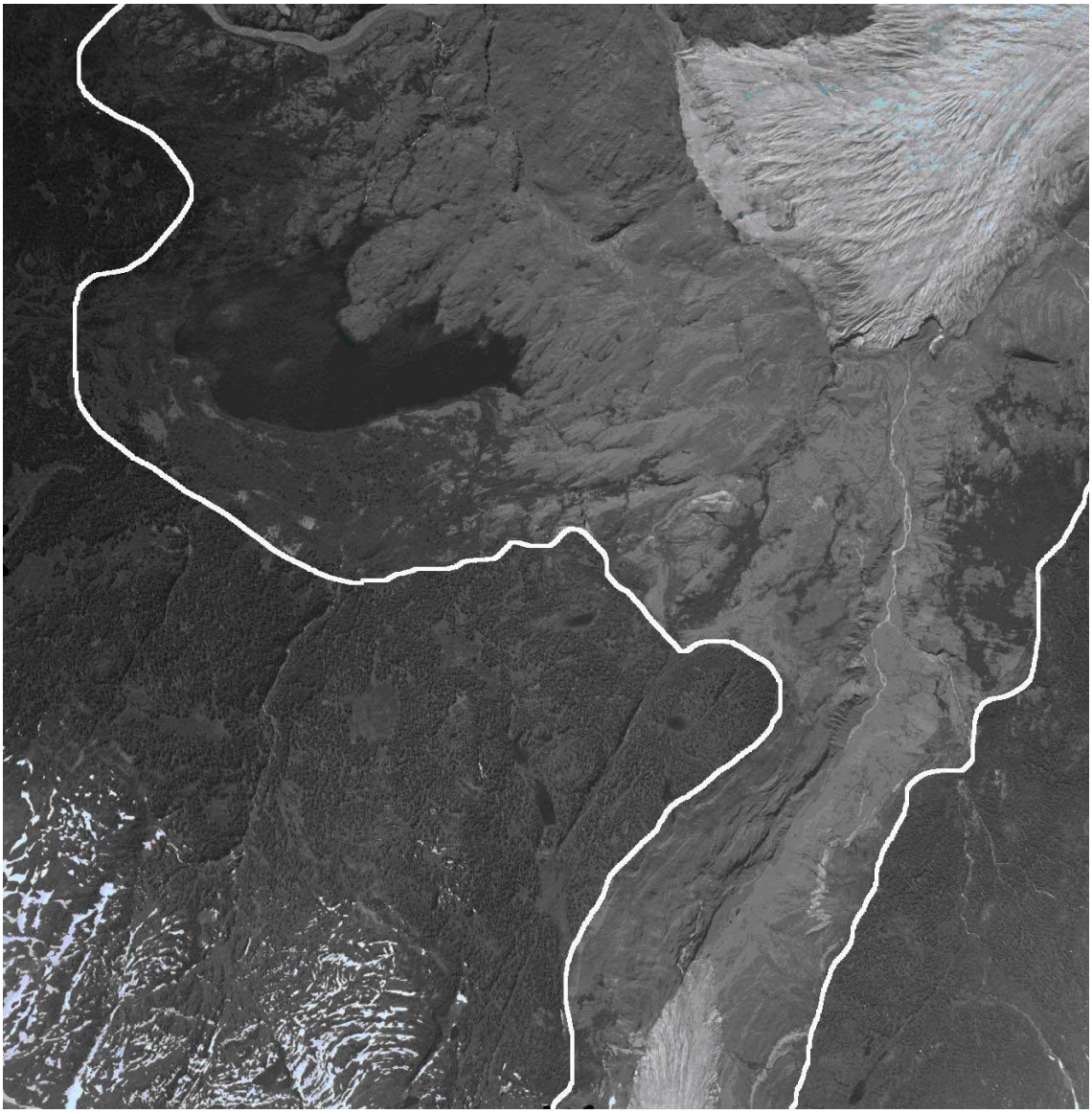

demarcated by a terminal moraine complex 2.5 km from the glacier terminus at 715 m asl. The moraine dams White Lake and is extensively colonized by sitka alder (*Alnus sinuata* [Regel] Rydb.; Figure 3.4). Both White Lake and White Glacier drain into the White River. Historical aerial photographs and field surveys show that from 1946 to 2007 the terminus of White Glacier retreated at rates varying from 51 to 10.3 m/yr (Table 3.1).

Figure 3.4: The White Glacier forefield, looking from White Glacier towards White Lake. The White Glacier forefield is heavily colonised by sika alder *(Alnus sinuata)*.

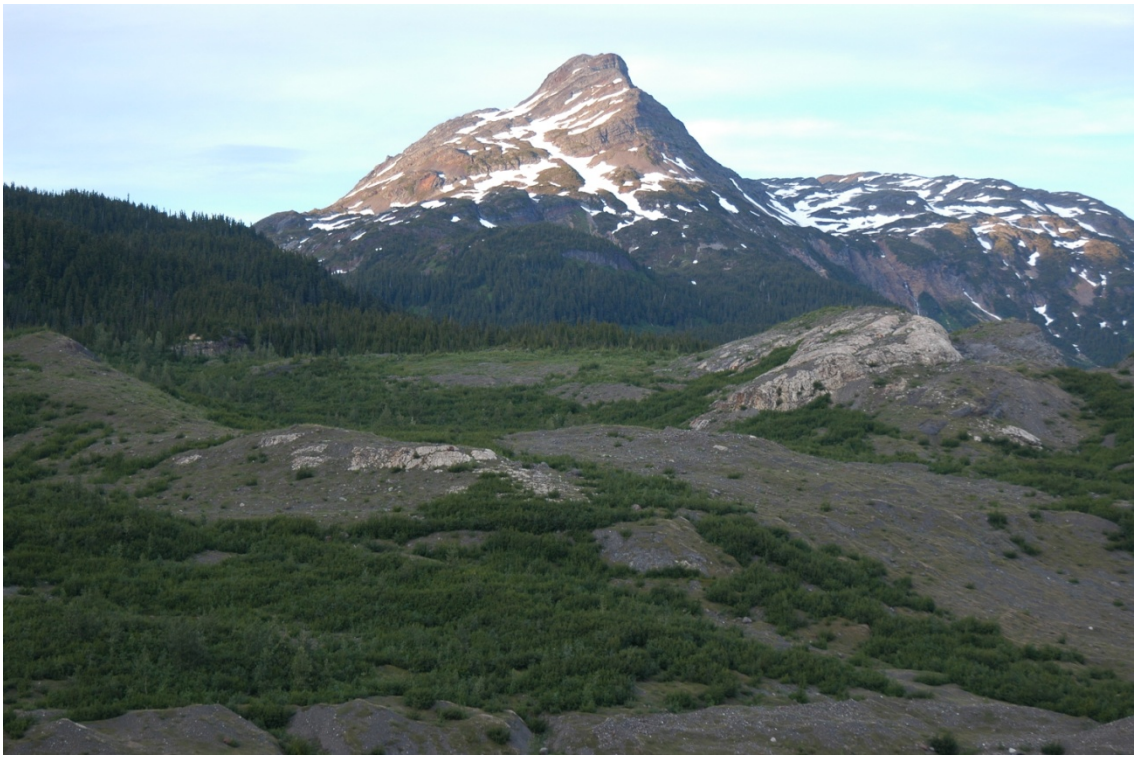

South Flat Glacier (Lat 55° 51’ N, Long 129° 27’ W; Figure 3.1) is a distributary of the larger Flat Glacier (*unofficial name*) that flows from the Cambria Icefield to drain into Flat River. South Flat Glacier spills south over the hydrological divide and flows into South Flat valley. Subglacial meltwaters from South Flat

Glacier flow south before joining the White River below White Glacier. The terminus position of South Flat from 1946 to 2007 retreated at rates varying from 29.8 to 6.3 m/year (Table 3.1).

As White Glacier advanced, retreated, and periodically blocked meltwater flowing downvalley from South Flat Glacier, it is likely that this glacially-dammed lake formed and drained a number of times. Aerial photographs from 1946 appear to show grounded icebergs north of White Glacier. Field investigations in 2008 found evidence suggesting the recent draining of a glacially-dammed lake (Figure 3.5).

Figure 3.5: The view from White Glacier in late-July 2007. In the foreground is showing the location of a recently drained glacially damned lake. This may correspond to the ice contact lake shown in Figure 3.6 (site 3), noted by Groves (1946).

Most of the White Glacier forefield is characterized by bare glacially-sculptured bedrock and isolated till units. An exception is the large area of water-logged and fluted sediments located immediately north of the snout of White Glacier in 2007 (Figure 3.4). Aerial photographs from 1946 indicate this area was the location of a small ice contact lake that had only recently drained when the site was first examined in 2007 (Figure 3.5). During geological investigations in the area between 1963 and 1964 (Grove 1973) a glacially dammed lake was observed close to the confluence of White and South Flat glaciers (Figure 3.6).

South Flat valley is characterized by prominent bedrock outcrops and extensive bedded sedimentary units. Cross-sections revealed in abandoned river channels show the latter consist of >10 m thick silt-dominated glaciolacustrine deposits, as well as interbedded units of steeply-dipping sand and gravel delta deposits (Figure 3.7). The sedimentary units terminate down valley adjacent to an interlobate moraine marking the confluent position of White and South Flat glaciers in the late LIA.

Figure 3.6: Geological map from Groves (1973). 1. White Glacier; 2. South Flat Glacier; 3. A small lake, ponded by White Glacier, and; 4. White Lake.

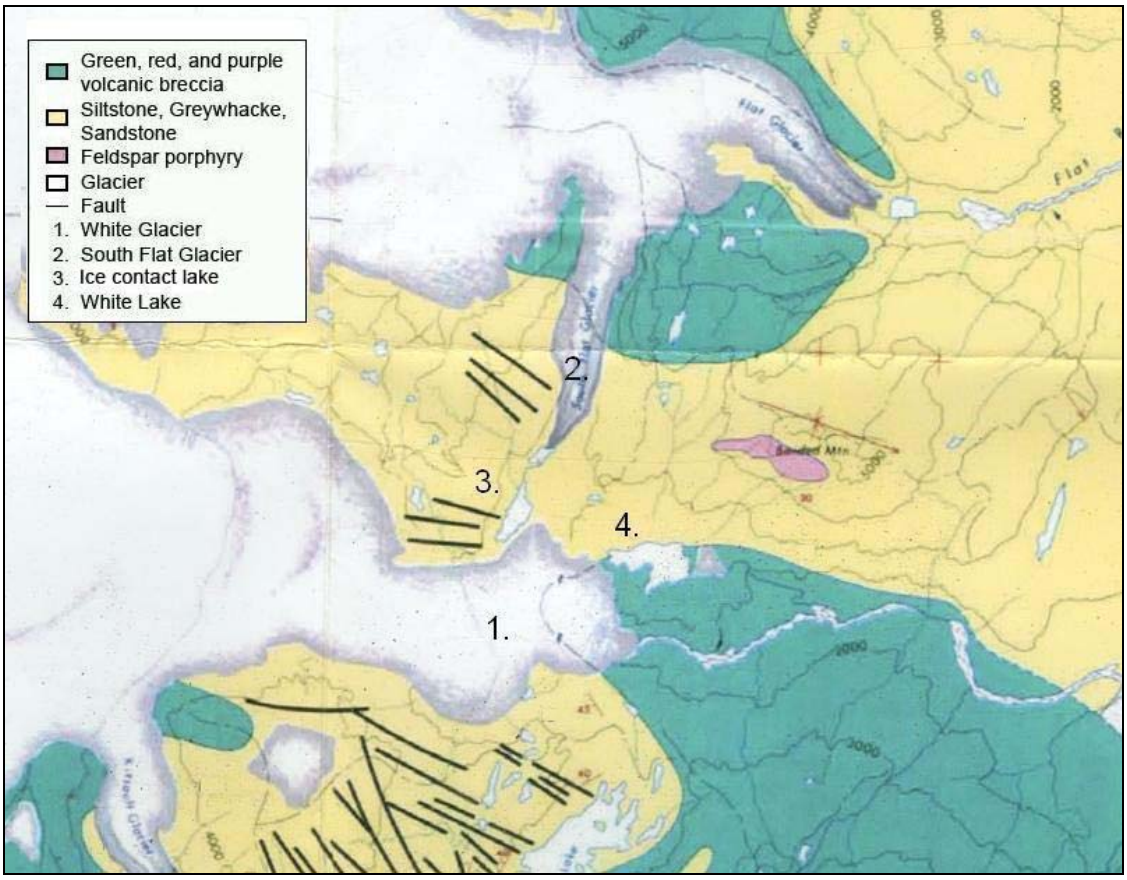

Figure 3.7: The view of South Flat valley and South Flat river. The white box highlights highlights the location of late-LIA prograded delta sediments.

3.4 Research Methods

Partially-buried subfossil stumps and detrital boles were exposed at a number of sites in the White and South Flat glacier forefields (Figure 3.2). A chainsaw was used to collect 'cookies' of wood. This sampling was designed to situate floating tree-ring series in time using a combination of dendroglaciological and radiocarbon dating methods (Luckman 1995; Smith and Lewis 2007b). Increment core samples were collected from a stand of mountain hemlock trees positioned above the terminus of South Flat Glacier in order to assign absolute dates to the tree-ring chronologies developed from the subfossil wood samples (Stokes and Smiley 1968).

3.4.1 Sample Preparation and Measurement

After air drying and mounting the samples were sanded to a fine polish at the University of Victoria Tree-Ring Laboratory. Once the ring boundaries were visible, the samples were scanned using a high resolution scanner and the total ring widths measured using WinDENDRO™ software to the nearest 0.01 mm. For series with narrow annual rings, the ring widths were measured with MeasureJ2X (VoorTech Consulting 2009) to the nearest 0.01 mm using a Velmex-stage equipped with a microscope and CCD video display.

The living tree-ring samples were first internally cross dated visually to narrow marker rings using CDendro software (Ver. 7.1, Cybis Elektronic & Data AB). Following visual cross dating, the International Tree Ring Database (ITRDB) software program COFECHA was used verify the cross dating using block correlations between each tree series and the master chronology (Holmes *et al.* 1986). COFECHA correlations were calculated using a 50-year segment length lagged successively by 25 years at a one-tailed 99% confidence level (Grissino-Meyer 2001). A living tree-ring chronology was constructed by using double detrending options in the ITRDB software program ARSTAN (Cook and Holmes 1986) to retain any low-frequency variability within the resulting chronology (Cook *et al.* 1990). To create a single dimensionless value for each growth year, each ring-width-index series was prewhitened using autoregressive and moving average models to remove any autocorrelation effects (Cook 1985; Biondi and Swetnam 1987).

Site-specific floating tree-ring chronologies were constructed from the subfossil samples following established cross dating protocols (Stokes and Smiley 1968) and CDendro software. An attempt was made to determine the absolute age of each floating chronology by cross dating to the standardized living chronology (Smith and Lewis 2007b). Where this failed, calibrated radiocarbon ages determined by CALIB 6.0 were assigned to the perimeter rings. Midpoints of the calibrated age range dates are reported, except in the case of multiple age intercepts where all possible ages are reported.

3.5 Observations

3.5.1 Dendrochronology

Twenty-seven ring width series from 17 individual trees were used to construct the local tree-ring chronology (Figure 3.8). The chronology spans 373 years (1635-2007) with a mean inter-series correlation of 0.548 and a mean sensitivity of 0.231 (Table 3.2). An EPS cutoff point was established at 1680 due to low sample depth prior to this (Wigley *et al.* 1984).

The duration and cross dating potential of the South Flat chronology was enhanced by including it within a regional master chronology constructed from UVTRL site chronologies previously collected at Surprise Glacier (1596 to 2007) and Windy Pass (1613 to 2004; Table 3.2). The three chronologies strongly cross date to form a chronology (n= 87 series) spanning 412 years (1596 to 2007; Figure 3.8). The EPS cutoff is at 1680, leaving the regional chronology with a mean inter-series correlation of 0.544 and an average mean sensitivity of 0.244.

Figure 3.8: Living tree-ring mountain hemlock (*Tsuga mertensiana*) chronology from the South Flat Glacier.

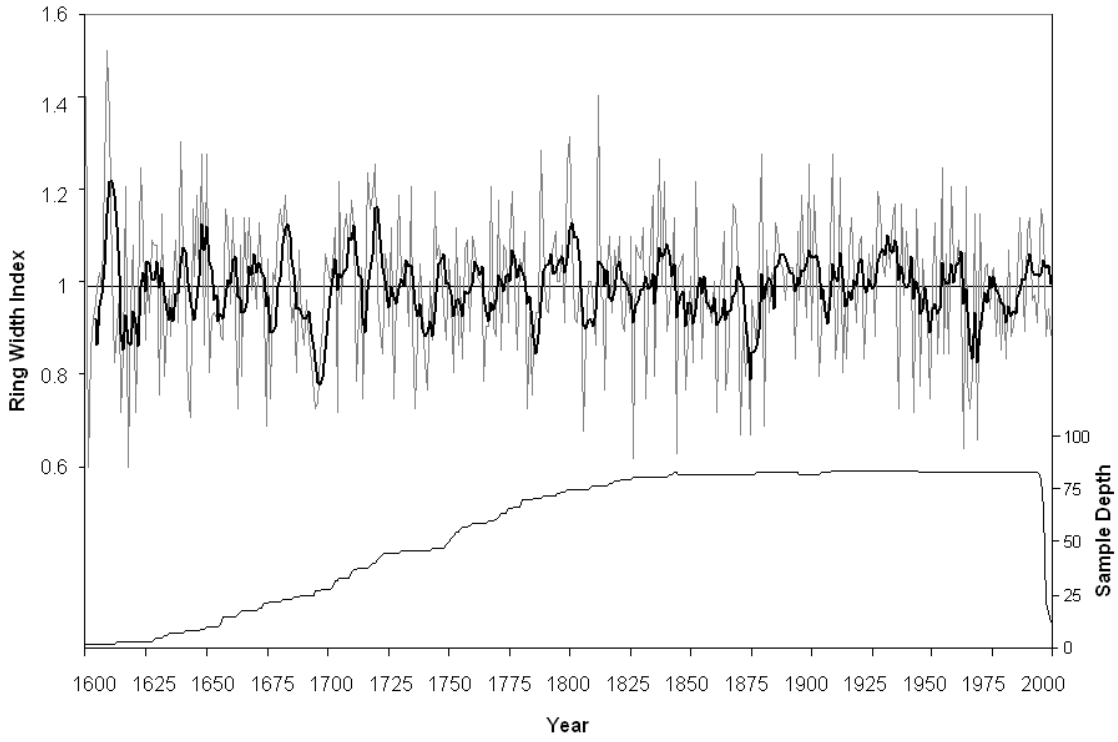

Table 3.2: Living tree-ring chronology statistics.

Site	Latitude	Longitude	Elevation (m asl)	Series mean first-order autocorrelation	Series mean sensitivity	Total Series length (years)
Surprise	56° 12’	129° 36’	910	0.535	0.211	408
Windy Pass	56° 06’	129° 30’	1090	0.595	0.271	391
South Flat	55° 49’	129° 29’	1035	0.548	0.231	373
Master	-	-	-	0.544	0.244	411

3.5.2 Dendroglaciology

3.5.2.1 Site 1

Site 1 is located within a 25 m high south-west facing cutbank positioned adjacent to an abandoned river channel in the White Glacier forefield ca. 750 m from the 2007 terminus position (Table 3.3). It is distinguished by three stratigraphic units (Figure 3.9). The lower most unit (Unit 1A) consists of a massive 10 m thick matrix-supported till with an upper surface truncated by a laterally extensive wood mat. The mat extends for ca. 15 m and contains glacially-transported broken bole, branch and stump fragments inter mixed with till. This wood mat is overlain by a weakly-bedded 7 m thick till unit (Unit 1B) capped by an orange-stained sedimentary horizon dipping up-slope 20^0 west-east. At this juncture a thin composite horizon consisting of small detrital wood pieces and

Table 3.3: Subfossil study sites at White Glacier and their associated UTM coordinates and elevation values.

Site Name	Lat. (N)	Long. (W)	Elevation (m asl)
1	55° 48’ 573”	129° 29’ 121”	653
2	55° 48’ 630”	129° 29’ 133”	673
3	55° 48’ 205”	129° 28’ 457”	679
4	55° 48’ 230”	129° 28’ 377”	685
5	55° 48’ 260”	129° 27’ 466”	660
6	55° 48’ 393”	129° 29’ 495”	875
7	55° 49’ 248”	129° 28’ 530”	789
8	55° 49’ 400”	129° 28’ 500”	865
9	55° 49’ 307”	129° 28’ 571”	818 - 851

Figure 3.9: Looking north towards site 1. Three units are highlighted: a 10 m thick matrix-supported till (1A), wood samples taken from the mat (Sample 01_01) date to 605 A.D. This unit is overlain by a 7 m thick till unit (1B) capped by an orange-stained sedimentary horizon. Resting on the surface of this horizon is a 7 m thick till unit (1C) whose upper surface features small north-west trending glacial flutes.

gravels extends across the cut face. Resting on the surface of this horizon is a 7 m thick till unit (Unit 1C) whose upper surface features small-scale north-west trending glacial flutes.

Cross-sections were collected from 4 boles found at the boundary between Units 1A and 1B (Figure 3.9). Tree ring counts from pith to perimeter indicate the trees were from 126 to 160 years old when they were killed. A calibrated calendar date of 605 A.D. was assigned to the outermost perimeter rings (n = 98) of sample 01_01 (Table 3.4). Crossdating of this sample with two others from Site 1 (01_02

and 01_03; Table 3.5) led to the construction of an 221 year-long floating chronology extending from ca. 247 to 468 A.D. (Chronology 1, Table 3.5).

Table 3.4: Summary of conventional age radiocarbon dated samples from White and South Flat Glaciers.

Sample ID	BETA ID	Species	Perimeter rings	^{14}C age years BP	2σ Calibration age range (A.D.)	2σ Calibration date BP	Assigned age (years A.D.)
01_01	262876	mh	98	1460 ± 40	550 - 660	1400 - 1290	605
02_03	262877	mh	104	1550 ± 40	420 - 600	1530 - 1350	510
03_10	273508	saf	34	1360 ± 40	600 - 680	1350 - 1270	640
03_14	262878	mh	68	1530 ± 40	420 - 610	1520 - 1340	515
05_02	262879	saf	76	1360 ± 50	570 - 680	1380 - 1270	625
06_04	250505	saf	62	1400 ± 40	590 - 670	1360 - 1280	630
07_01	250501	mh	120	1280 ± 50	650 - 880	1300 - 1070	765
08_12	273508	mh	67	960 ± 40	1000 - 1160	950 - 790	1080
09_16	250503	mh	121	810 ± 40	1160 - 1280	790 - 670	1220
09_18	250504	saf	46	610 ± 60	1280 - 1430	670 - 520	1355

[a]saf, subalpine fir; mh, mountain hemlock. Species were identified by their gross anatomical characteristics (Hoadley 1990).
[b]All radiocarbon dates and 2σ ranges calculated by Beta Analytic Inc. using INCAL04.

3.5.2.2 Site 2

Site 2 is located at 673 m asl within a north-facing abandoned meltwater stream cut bank (Figure 3.10). Positioned 25 m upstream from Site 1, this section was located ca. 775 m from the terminus of White Glacier in 2008 (Figure 3.2; Table 3.3).

Table 3.5: The floating tree-ring chronologies created for this thesis and their conventional age dates assigned after unsuccessful cross-dating into the living tree-ring chronology. If the sample was used in the FMA Chronology (Figure 3.18), then the perimeter age date is recorded.

Sample No.	^{14}C age years (±2σ BP)	Number of rings	Correlation with master	Perimeter age (FMA Chronology)
Floating Chronology Site 1				
01_01A	1460 ± 40	122	0.292	
01_02A		160	0.232	468
01_02B		149	0.468	461
01_03B		91	0.354	417
Floating Chronology Site 2				
02_01A		179	0.321	488
02_01B		185	0.375	
02_02A		237	0.490	555
02_02B		185	0.625	511
02_03A	1550 ± 40	193	0.375	517
Floating Chronology Site 3				
03_10A	1360 ± 40	316	0.481	548
1 03_10B	1360 ± 40	314	0.409	548
03_11A		149	0.331	
03_11B		112	0.489	
03_02A		217	0.621	582
03_02B		217	0.545	582
2 03_03A		153	0.224	
03_06A		110	0.211	
03_06B		119	0.370	
3 03_14A	1530 ± 40	227	0.539	592
03_14B	1530 ± 40	199	0.539	560
Floating Chronology Site 4				
04_01A		110	0.546	
04_01B		94	0.790	
04_02A		89	0.610	634
04_02B		106	0.438	634
04_03A		167	0.353	
04_03B		167	0.313	
04_04A		93	0.521	
04_04B		99	0.595	
Floating Chronology Site 5				
05_01A		208	0.447	554
05_01B		205	0.422	552
05_02B		100	0.314	
Floating Chronology Site 6				
06_04A		63	0.786	559

	06_04B		63	0.619	
	06_08A		63	0.560	601
	06_08B		72	0.498	612
	06_09A		59	0.334	555
	06_09B		72	0.330	
Floating Chronology Site 7					
1	07_01A	1280 ± 40	456	0.425	
	07_01B	1280 ± 40	454	0.425	
2	07_02A		208	0.560	
	07_02B		206	0.644	
	07_04A		166	0.402	
	07_04B		181	0.250	
	07_05A		101	0.403	
	07_05B		105	0.594	
Floating Chronology Site 8					
	08_09A		114	0.209	
	08_10A		93	0.438	
	08_10A		95	0.566	
	08_11A		115	0.435	631
	08_11B		119	0.408	
	08_12A		60	0.570	
	08_12B		77	0.596	
Floating Chronology Site 9-lower					
	09_16A	810 ± 40	219	0.468	
	09_16B	810 ± 40	180	0.468	
Floating Chronology Site 9-upper					
	10_17B		113	0.336	
	09_18A	610 ± 60	119	0.643	
	09_18B	610 ± 60	133	0.624	

The site consists of a 20 m thick section of till and enclosed pockets of 2 to 3 m long boles with masticated surfaces. Cross-sections were collected from 4 mountain hemlock boles positioned 12 and 17 m from the channel base (Figure 3.10). The samples contain from 185 to 237 annual rings, and three cross date to form a 250 year long floating chronology (Chronology 2, Table 3.5). Radiocarbon

dating of 104 perimeter rings from sample 02_03 indicates the chronology extends from ca. 305 to 555 A.D. (Table 3.5).

Figure 3.10: Looking south towards site 2. Two white boxes highlight the location of the two pockets of sampled wood with sample 02_03 dated to 510 A.D.

3.5.2.3 Site 3

Site 3 is located 1 km east of the 2007 terminus position of White Glacier at 679 m asl (Figure 3.2; Table 3.3). The site is positioned below the proximal face of a 10 m high glacially-eroded bedrock outcrop (Figure 3.11). The colluvial footslope consists of a diamicton intermixed with partially-buried broken and fragmented bole segments up to 6 m in length. The sediment and woody debris appears to have

eroded from the bedrock face following retreat of the glacier from the site prior to 1949 (Figure 3.11).

Figure 3.11: East towards the exposed wood at site 3 against bedrock. Samples were located at the base of a 10m high bedrock outcrop in a diamicton intermixed with partially buried and buried bole segments up to 6m in length. Two radiocarbon ages were assigned to this site: 640 A.D. (Sample 03_10; within white box) and 515 A.D. (Sample 03_14; not shown on photograph).

Fifteen cross-sections were collected from small woody fragments and detrital boles. Dendrochronological analysis led to the construction of two chronologies. A subalpine fir chronology (3-1) was created from samples ranging in age from 120 to 149 years (Table 3.5). Extending over a 316 yr interval, the

chronology is anchored by the perimeter wood dating of sample 03_10 to 640 A.D. (Table 3.4).

A mountain hemlock chronology was created from samples found intermixed at Site 3 with those incorporated into Chronology 3-2. The chronology includes three series with between 119 to 217 annual rings (Chronology 3-2; Table 3.5), and extends over a 217 yr period. As no radiocarbon date is directly assigned to any sample within this chronology, it is assumed that the series included in this chronology came from trees killed at the same time as those incorporated into Chronology 3-1, indicating that Chronology 3-2 extends from 232 to 548 A.D. (Table 3.5).

3.5.2.4 Site 4

Site 4 is located 25 m west of Site 3 in a small mossy area found on the east face of a prominent bedrock outcrop at 675 m asl. The site was ice free prior to 1946 and contains 0.5 to 1 m long bole segments (99 to 110 rings) pressed into a small pocket of organics.

Cross-sections were collected from five samples. Three subalpine fir samples cross date to form a floating 110 yr long chronology (Chronology 4, Table 3.5). The chronology cross dates to Chronology 3-3 indicating that the trees at Site 4 were killed ca. 515 A.D. (Table 3.5).

3.5.2.5 Site 5

Site 5 is located ca. 20 m north of sites 3 and 4, in an 6 m deep east-west facing bedrock gully at 660 m asl (Figure 3.12). A large accumulation of broken and

fragmented detrital wood was located in the gully, where it appears to have been pushed as White Glacier advanced over the surrounding bedrock surface. The site was exposed sometime prior to 1946.

Although most of the wood at Site 5 was rotted and in poor condition, cross sections were collected from two bole segments with 100 (05_02) and 208 (05_01) rings (Table 3.5). These samples cross date to form a 205 yr long chronology (Figure 3.12). A perimeter age assigned to 05_01 indicates the trees were killed in ca. 625 A.D. (Table 3.4).

Figure 3.12: Looking south across the exposed debris at site 5. The gully ran for 20 m north to south and was 6 m deep. Sample (05_01) indicates these trees were killed ca. 625 A.D.

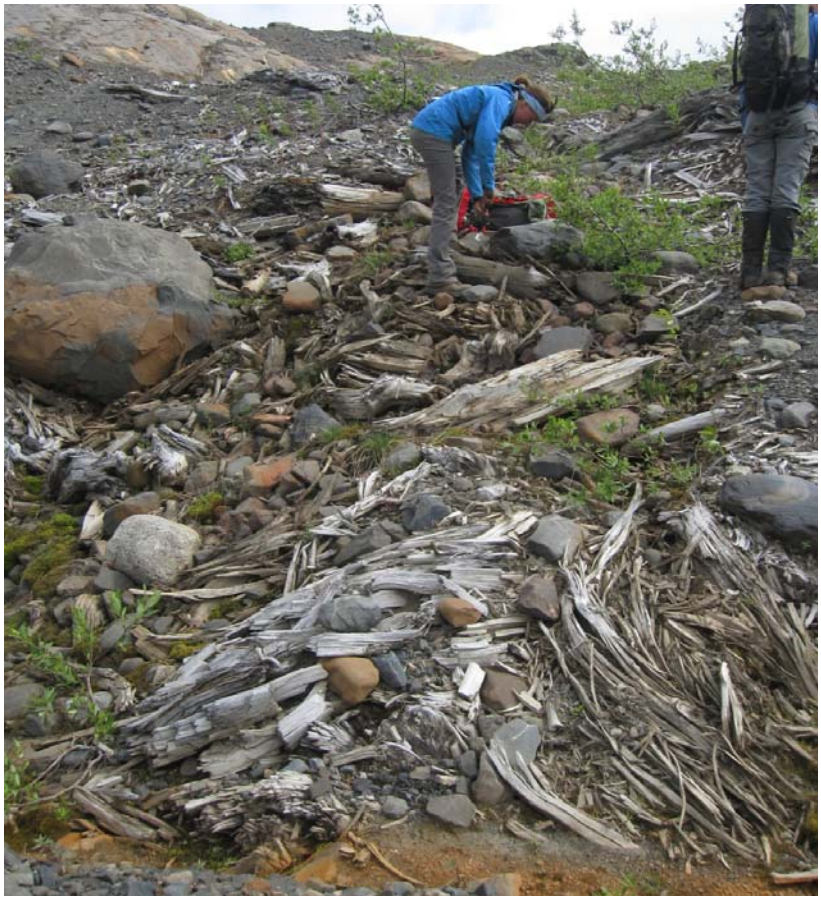

3.5.2.6 Site 6

Site 6 is found north of White Glacier at 1002 m asl on the west side of a prominent bedrock ridge separating the White and South Flat glacier forefields (Figure 3.13). The site was ice free by 1985 and consists of a broad pocket of till deposited by White Glacier in a gully surrounded by steeply-sloping bare bedrock surfaces (Figure 3.13). A small ephemeral stream draining the upper bedrock ridge flows through the alder-filled gully and is actively eroding the sediments.

Figure 3.13: Looking north from White Glacier to site 6. Wood was sampled from detrital wood in an alder gully. The white box shows the location of the 5 samples logs killed ca. 640 A.D.

Partially buried 2 to 7 m long boles and woody detritus were located within and on the till (Figure 3.13). Cross-sections retrieved from the five largest boles have from 63 to 72 annual rings. A floating chronology was constructed from three

samples creating an 81 year long floating chronology (Table 3.5). Perimeter rings from one sample (06_04) indicate the trees at Site 6 were killed ca. 640 A.D. (Table 3.4).

3.5.2.7 Site 7

Site 7 is located in the South Flat valley floor at 762 m asl, 2 km downstream from the 2007 terminus of South Flat Glacier (Figure 3.14). Following the retreat of the glacier from the site prior to 1946, the river incised through over 70 m of till and glaciolacustrine sediments to expose numerous broken and toppled boles that

Figure 3.14: Looking south towards White Glacier at Site 7. The white box highlights the *in situ* Sample 07_01 (765 A.D.). Disks were taken from samples within the river channel and in an adjacent deposit to the west of the river channel to form Chronologies 7-1 and 7-2.

exceed 7 m in length. Samples were collected from 5 to 7 m long boles. Containing from 108 to 205 annual rings, the samples were in poor condition and did not cross date. A single *in situ* stump (07_01) with 456 annual rings was located along the channel bank of South Flat River (Figure 3.14). Radiocarbon dating of the outermost 120 rings indicates the tree died ca. 765 A.D. (Table 3.4).

3.5.2.8 Site 8

Site 8 is found adjacent to South Flat River at 820 m asl. The site is located immediately downstream of a prominent bedrock gorge 900 m from the terminus of South Flat Glacier (Figure 3.2; Table 3.3). Adjacent to the west side of the channel is a 25 m thick exposure of steeply-dipping laminated sands and gravels capped by till. The latter extends upwards to a non-conformable contact with fine-grained horizontally bedded rythmites (Figure 3.15 and 3.16).

Numerous woody fragments and bole segments were exposed within the upper section of the lower laminated unit. Cross-sections were collected from five small logs with between 59 to 117 rings. Radiocarbon dating of the outermost 67 rings of sample 08_11 indicates the tree died ca. 1080 A.D. (Table 3.4).

Figure 3.15: The steeply-dipping laminated sands and gravels capped by a till at site 8. Sample 08_11 indicates than the trees in this deposit were killed ca. 1080 A.D.

Figure 3.16: Bedded fine-grained rythmites at site 8 located beside a prominent bedrock gorge 900 m from the 2007 terminus of South Flat Glacier.

3.5.2.9 Site 9

Site 9 refers to a 60 m high vertical cross-section located ca. 50 m above Site 7 (Figure 3.2; Table 3.3) consisting of a horizontally-bedded laminate unit with alternating units of gravels and silty-sands. Woody horizons were found at the base of the unit at 840 m asl, at 860 m asl, and were visible, but not accessible, in the uppermost section of the unit at 900 m asl (Figure 3.17). The woody horizon appears to be matched by equivalent units visible on the other the side of the valley.

Figure 3.17: Sample 9_16 at site 9 (lower), radiocarbon dated to ca. 1220 A.D. Site 9 consisted of three woody horizons, at 818 m asl (lower), 851 m asl (middle; dated to 1355 A.D. and a third horizon (upper) that was inaccessible at around 900 m asl. These three woody horizons appear to be matched with equivalent units visible on the west side of the valley, highlighted with three white lines.

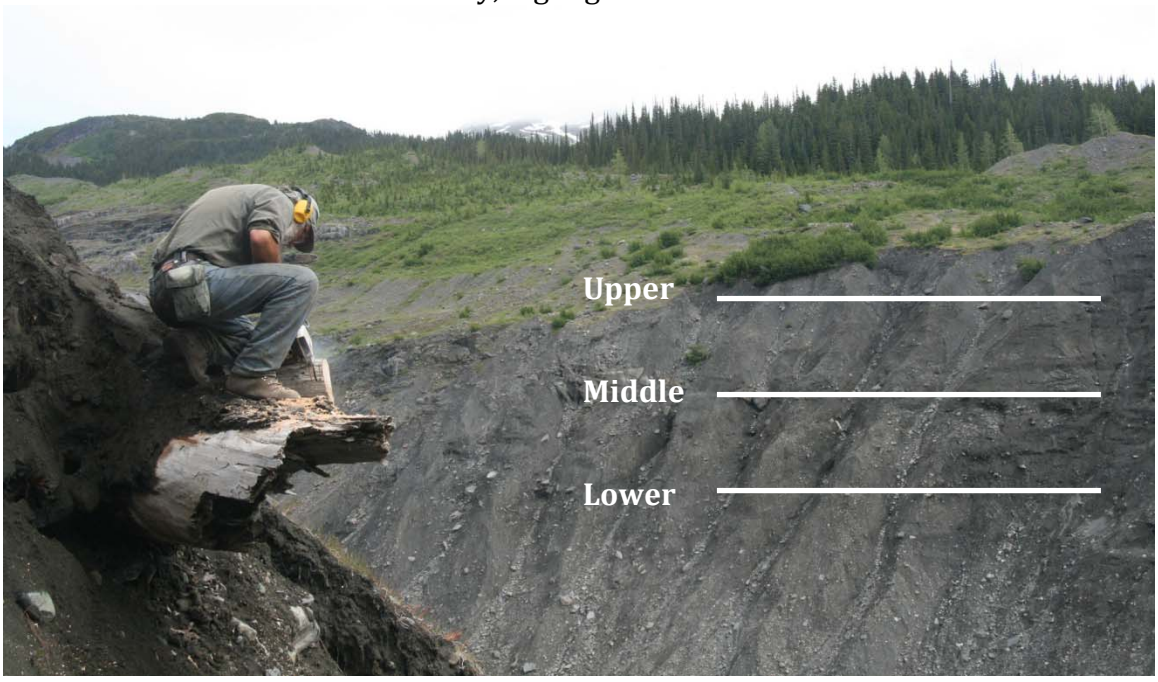

Three cross-sections were collected from boles found at the base of the section. They contain between 130 and 219 annual rings, but do not cross date

likely due to the prevalence of reaction wood within the samples. Perimeter wood from 09_16 (219 growth rings) indicates it was killed in 1200 A.D. (Table 3.5).

Cross-sections were collected from woody detritus found in the middle of the section at 860 m asl (Figure 3.16). Samples from two down-valley oriented bole segments (0.5 and 1 m in length) contain 113 and 133 rings (Table 3.5). Radiocarbon dating indicates that 09_18 was killed ca. 1355 A.D. (Table 3.4).

3.6 Results

Twelve site-specific floating chronologies were created and four were anchored in time by radiocarbon ages on multi-ring perimeter wood samples (Table 3.4; Table 3.5). In an attempt to absolutely date the floating chronologies each was compared to the regional living mountain hemlock chronology. The cross dating was unsuccessful and indicates the subfossil samples were all killed prior to 1596.

Following this an attempt was made to cross date the floating chronologies to one another. Seven of the floating chronologies successfully cross date and were combined to form the 'Cambria' chronology (Table 3.5; Figure 3.18). The Cambria chronology spans a 393 year interval and includes radiocarbon-dated samples that indicate trees included in the chronology were killed between 251 to 664 A.D. (Figure 3.18).

Figure 3.18: First Millennial Advance Chronology anchored by conventional radiocarbon date from sample 03_10 (Table 3.5). The chronology consists of samples from the White Glacier forefield, South Flat Valley and the Todd Icefields (from Jackson *et al.* [2008]). The chronology extends from 251 – 664 A.D. (393 years) and consists of 38 tree-ring records.

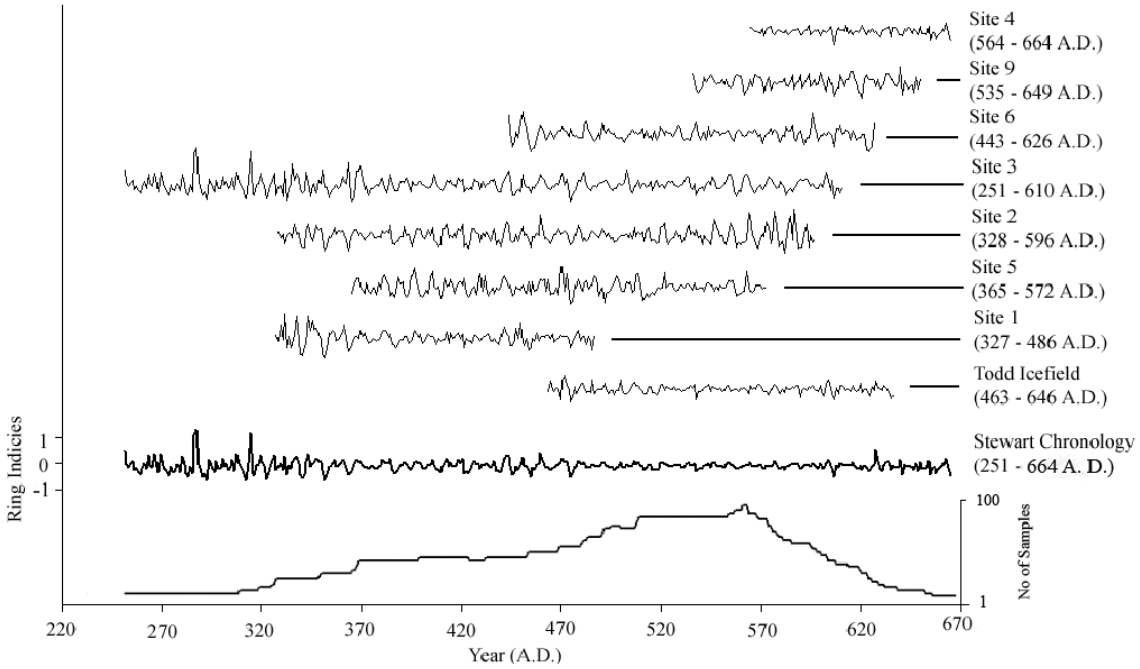

The floating 'Cambria' chronology was compared to chronologies constructed from subfossil samples previously collected in the nearby Todd Icefield area (Jackson *et al.* 2008). Fifteen samples cross date to the Cambria chronology and were used to form a combined 'Stewart' chronology (Figure 3.18). The Stewart chronology contains 38 tree ring records, spans a 393 year period, and includes 6 radiocarbon dated perimeter wood samples (Table 3.5). Perimeter wood from 03_10 records the most recently killed sample (600 - 680 A.D.; Table 3.5) and was used anchor to the chronology (Figure 3.18). This adjustment resulted in the kill-dates of the five remaining radiocarbon samples falling within 2σ of the midpoint of the calibrated age range (Table 3.4).

3.6.1 Interpretation

Field investigations are used to document an FMA advance of White Glacier from ca. 250 to 650 A.D.; as well as the early LIA interactions of both South Flat and White glaciers. No evidence was found to describe glacier activity earlier in the Holocene, this despite nearby records detailing extensive early and late Tiedemann-age Advances (Clague and Matthews 1992; Jackson *et al*. 2008).

Evidence from the White Glacier forefield (sites 1 – 6) describes an FMA ice front advance from 486 to 664 A.D. into a standing forest composed of mountain hemlock and subalpine fir trees. Shortly before 486 A.D. the glacier crossed South Flat River and began moving up the west-facing valley side overwhelming trees (Figure 3.19). The glacier reached Site 1 in 486 A.D. and deposited wood at Site 2 in 596 A.D. The minimum rate of advance over this interval was 4.4 m/yr. Following this the snout of White Glacier continued to thicken and extend up the valley site, reaching Site 3 by ca. 610 A.D. At about the same, White Glacier was pushing woody detritus into the gully at Site 5. The glacier snout reached Site 4 by 664 A.D., having advanced up the bedrock slope from the vicinity of Site 3 at a minimum of 0.4 m/yr.

The distal position of the woody detritus at Site 4 indicates that White Glacier advanced over the ridge crest and was flowing downslope toward White Lake after 664 A.D. No dendroglaciological evidence was recovered describing the maximum extent of this advance, the minimum estimate can be derived by extrapolating the ice surface profile at this time. Cross dating established that

Figure 3.19: The advance of White Glacier killed this tree (within the white box) prior to 486 A.D. As White Glacier advanced into and overwhelmed a standing forest, it pushed the tree against this bedrock. The tree was exposed after 2001.

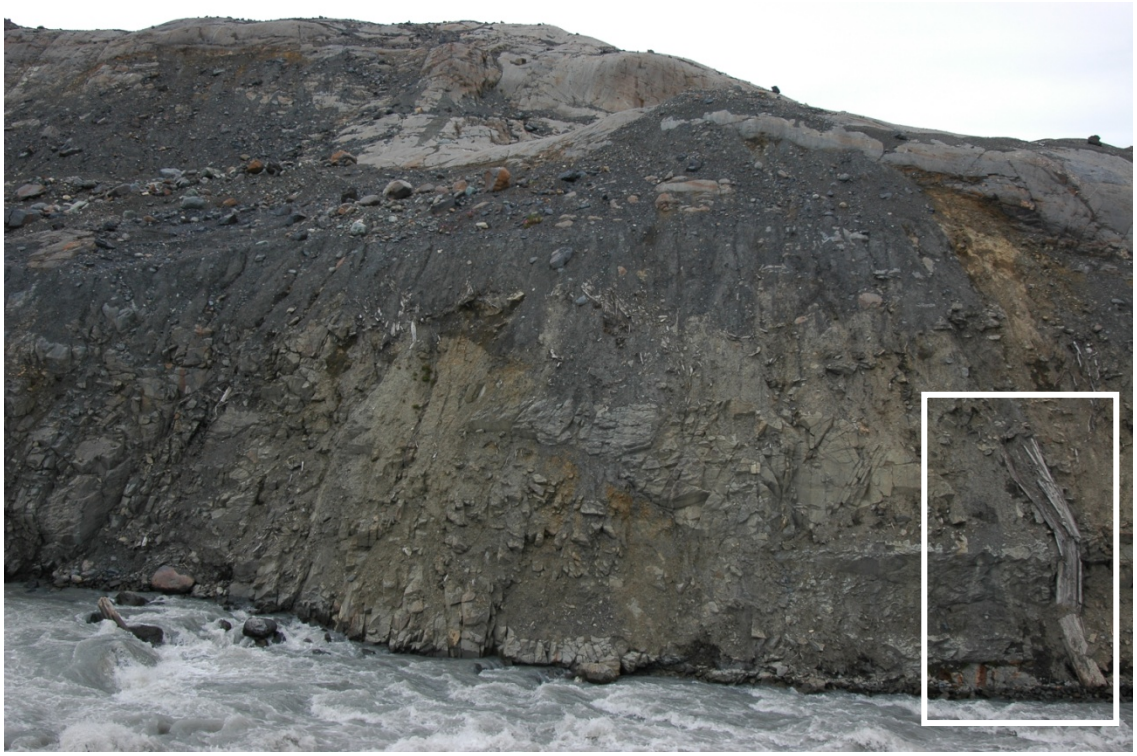

White Glacier was killing trees at both sites 5 (660 m asl) and 6 (915 m asl) ca. 625 A.D. As the two sites were located on opposite sides of South Flat valley (Figure 3.2) the cross valley ice surface profile at that time can be reconstructed (Figure 3.20). Assuming that a similar west-east surface slope exists (20˚), White Glacier would have likely extended as far downvalley as the western edge of White Lake (Figure 3.20).

FMA expansion and thickening of White Glacier eventually resulted in an ice dam that blocked the drainage of meltwater flowing from South Flat Glacier down South Flat valley (Figure 3.20). The timing and nature this ice dam is constrained by the *in situ* stump located at Site 7 (07_01; Figure 3.14). Killed when submerged

by proglacial lake water in 765 A.D. (Figure 3.21), the tree was eventually engulfed by laminated glaciolacustrine sediments and then overtopped by prograding delta sediments as South Flat Glacier advanced downvalley. Abandoned bedrock channels at ca. 800 m asl indicate that water from the lake spilled over the intervening ridge to White Lake at a late high elevation stage (Figure 3.21). The existence of an ice dammed lake in 765 A.D., persisting long enough for thick sedimentary units to accumulate, indicates the glacier remained in this advanced position until sometime after 800 A.D. Wood fragments contained within the lower deltaic unit at Site 8 indicate the lake may have persisted until 1080 A.D.; although it seems more likely this deposit is associated with ice blockage resulting from the LIA advance of White Glacier.

The initiation of LIA glacier activity at South Flat and White glaciers is recorded by detrital wood found buried within the thick unit of glaciolacustrine deposits that unconformably overlie FMA-aged sediments at site 9. The large bole segments recovered within alternating sand and gravel units at the base of the unit (840 m asl) are interpreted to record a proglacial subaerial setting (08_12; Figure 3.22). Overlying this unit is a thick unit of coarsely laminated sand facies that records sedimentation in a shallow ice- or moraine-dammed lake associated with the extension of White Glacier into South Flat valley (Figure 3.15). Broken bole fragments dating to 1355 A.D. at 860 m asl are oriented downvalley and record flows originating from South Flat Glacier.

Figure 3.20: A schematic diagram of the ice surface profile of White Glacier: (A) during the FMA advance at 515 A.D., based on the cross-dating of detrital wood from site 4; and (B) during the late LIA, based on the location of the terminal moraines.

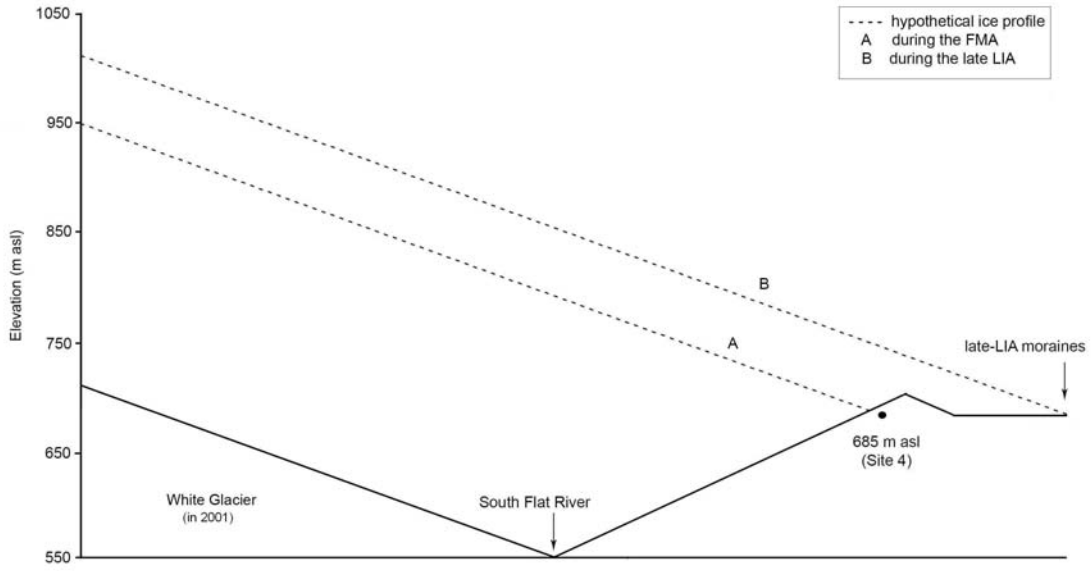

Figure 3.21: Schematic of the expansion of White Glacier and the subsequent interaction of White Glacier with South Flat Glacier between ca. 600 A.D. to the early Little Ice Age. In panel 1, the glacier is advancing to site 3 with South Flat river flowing beneath the glacier. In panel 2, the glacier has thickened sufficiently to force the ponding of a lake, killing sample 07_01 at site 7. South flat river subsequently flows around White Glacier. Panel 3 depicts the advance of South Flat Glacier, causing the formation of a prograding delta, deposition of sediments and death of trees at site 9. White and South Flat glacier are not confluent until the late Little Ice Age (panel 4), where all of the South Flat valley and White Glacier forfield is covered with glacial ice.

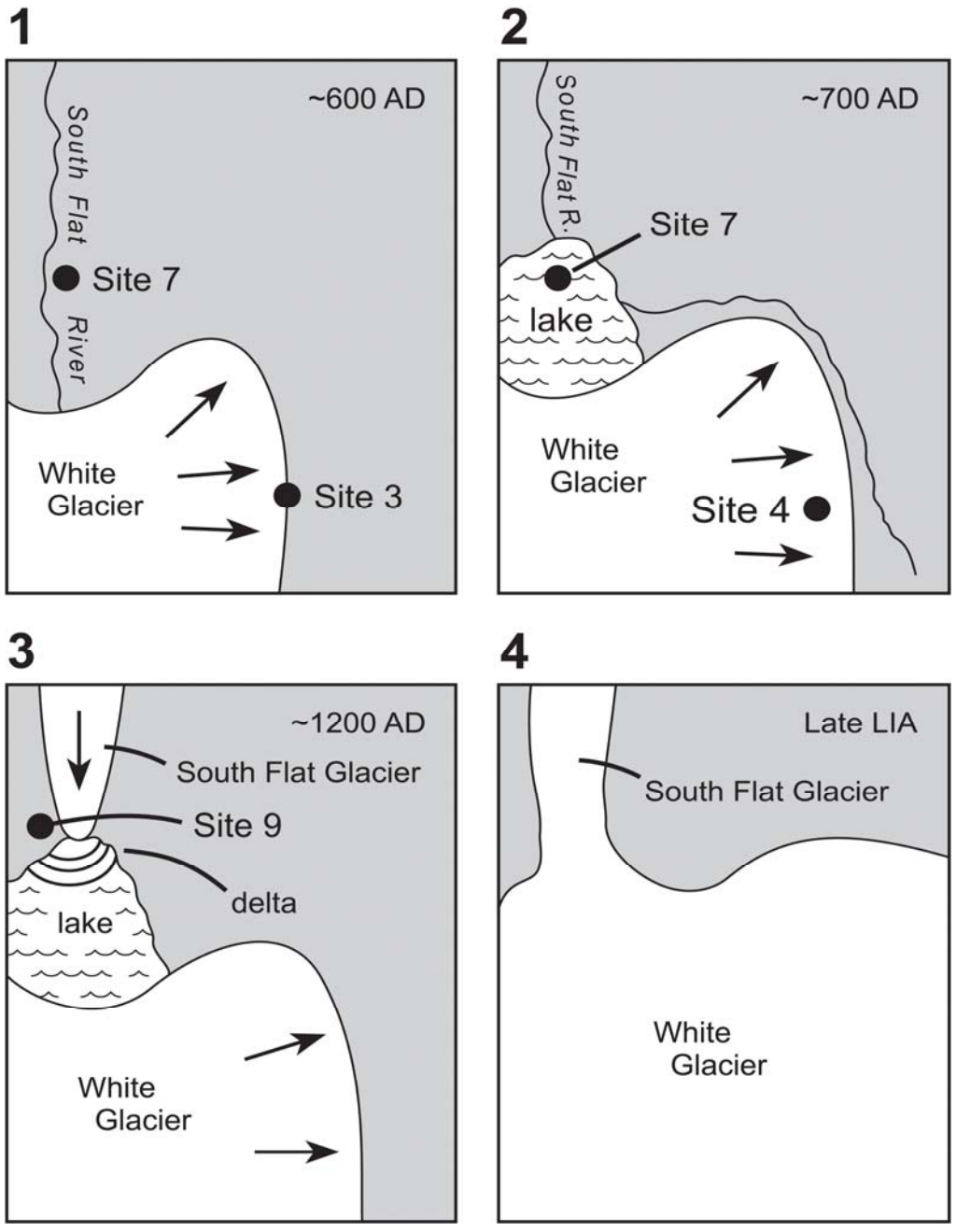

During this time, South Flat valley extended south, with White Glacier extending north into the South Flat valley. Overlying this unit are coarsening upward glaciofluvial units directly associated with the late-LIA moraines. The glaciers separated prior to 1949 (Figure 3.21 and 3.3). White Glacier continued to straddle South Flat River until after 2001 and there is evidence for the filling and drainage of a succession of short-lived ice damned lakes.

Figure 3.22: Looking up the South Flat valley. Sample 07_01 (765 A.D.) from site 7 is highlighted with a white box. Site 9 encompasses three woody horizons: The lower horizon (1220 A.D.; sample 09_16), middle horizon (1355 A.D.; 09_18), and an undated upper horizon. These three woody horizons appear to be matched with equivalent units visible on the west side of the valley (see Figure 3.17).

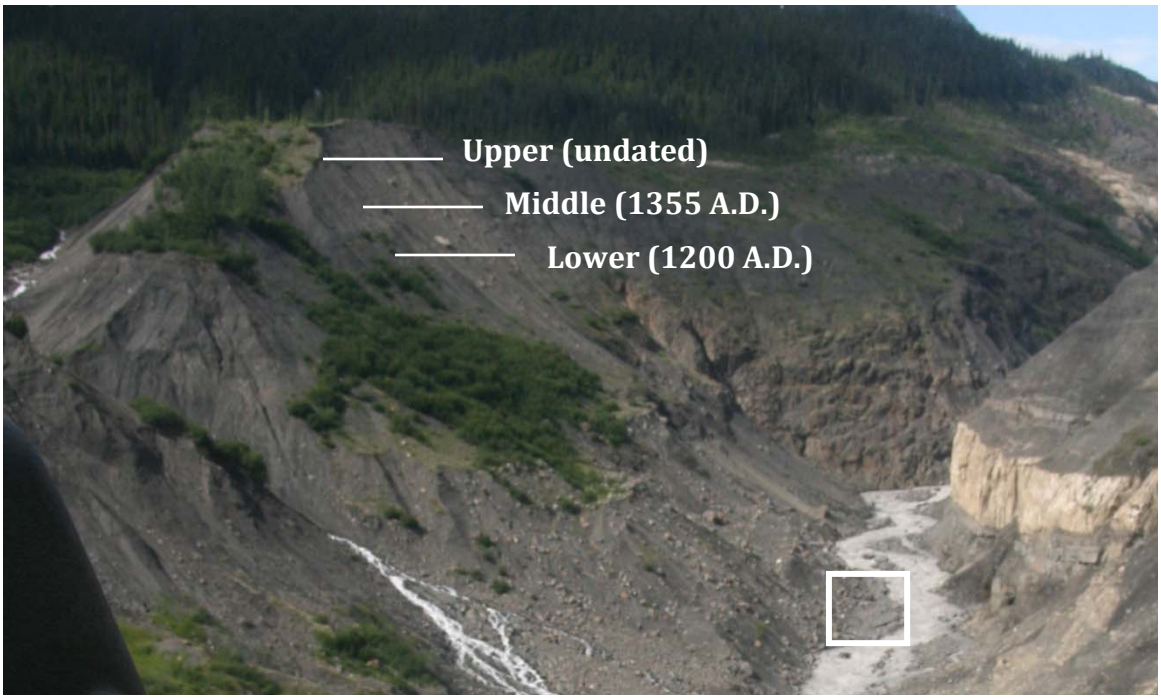

3.7 Discussion and Synthesis

Although previous research in the region indicates the FMA is distinguished by an early (375 A.D.) and late (605 A.D.) phase (Jackson *et al.* 2008), these investigations provide evidence for only a single continuous advance of White Glacier. The dendroglaciological findings from the site describe the advance of White Glacier in South Flat valley before 486 A.D. Over the following 250 years or so a gradual thickening of the glacier eventually blockaded the valley and led to the creation of an ice contact lake before 765 A.D. Related overflow channels carved into the bedrock interfluve drain toward White Lake. Thick bottomset and delta foreset sedimentary units describe an interval of sustained infilling of the lake that persisted until after 800 A.D. White Glacier appears to have thinned sufficiently before 1080 A.D. to allow the lake to partially drain around or beneath the glacier snout. Following this White Glacier readvanced and by 1080 A.D. blocked South Flat valley to create a second ice-contact lake that persisted until after 1355 A.D. Overlying till deposits indicate that South Flat and White glaciers were confluent in South Flat valley following this; a state that may have persisted until toward the end of the LIA in the last century.

The reconstructed FMA and LIA glacial history of South Flat and White glaciers is comparable to that reported at other sites in the region. Laxton (2005) and Jackson *et al*. (2008) report that several glacier fronts were advancing and expanding down valley from 230 to 650 A.D. in the nearby Todd Icefield. Clague and Mathews (1992) note that Frank Mackie Glacier was in an advanced state from

320 to 570 A.D. In the Andrei Icefield area, 150 km northwest of the study site, Forrest Kerr and Scud glaciers were actively advancing into standing forests at ca. 460 A.D. (Lewis and Smith 2005). Further afield in Alaska, coeval FMA kill dates have been found at Beare Glacier (Johnson *et al.* 1997) and Icy Bay Glacier (Barclay *et al.* 2006) from 420 – 670 A.D..

The early-LIA activity of South Flat and White glaciers appears to be contemporaneous with glacier activity documented in the Todd Icefield area at ca. 960 A.D. (Spooner *et al.* 2005) and ca. 1390 A.D. (Jackson *et al.* 2008). Corresponding glacier advances have been documented in the Stikine area at Scud Glacier at ca. 1380 A.D. (Ryder, 1987). At Tebenkof Glacier in southern Alaska, a comparable early LIA advance was underway at about 1320 A.D. (Barclay *et al.* 2009)

The apparent regional synchronicity of the FMA and early-LIA advances prompted an examination of the low and high frequency variability within the two tree-ring records constructed as part of this study. To highlight temporal rhythms retained within the subfossil and living chronologies, an interactive wavelet analysis[2] with a Gaussian 2 function and a 10% white noise reduction was completed.

Figure 3.23 illustrates the outputs from the wavelet analyses. Both chronologies retain a repetitive 8-year event thought to be associated with climate forcing mechanisms described by the El Niño Southern Oscillation (ENSO). This mode of variability persists throughout the duration of the live chronology (Figure

[2] http://paos.colorado.edu/research/wavelets; (Torrence and Compo 1998)

Figure 3.23: The wavelet power spectrum for the (a) Live Chronology, and; (b) the Stewart Chronology. The contour levels are chosen so that 75%, 50%, 25%, and 5% of the wavelet power is above each level, respectively. The cross-hatched region is the cone of influence, where zero padding has reduced the variance. Black contour is the 15% significance level, using a white-noise background spectrum. (c) The global wavelet power spectrum (black line). The dashed line is the significance for the global wavelet spectrum, assuming the same significance level and background spectrum as in (b).

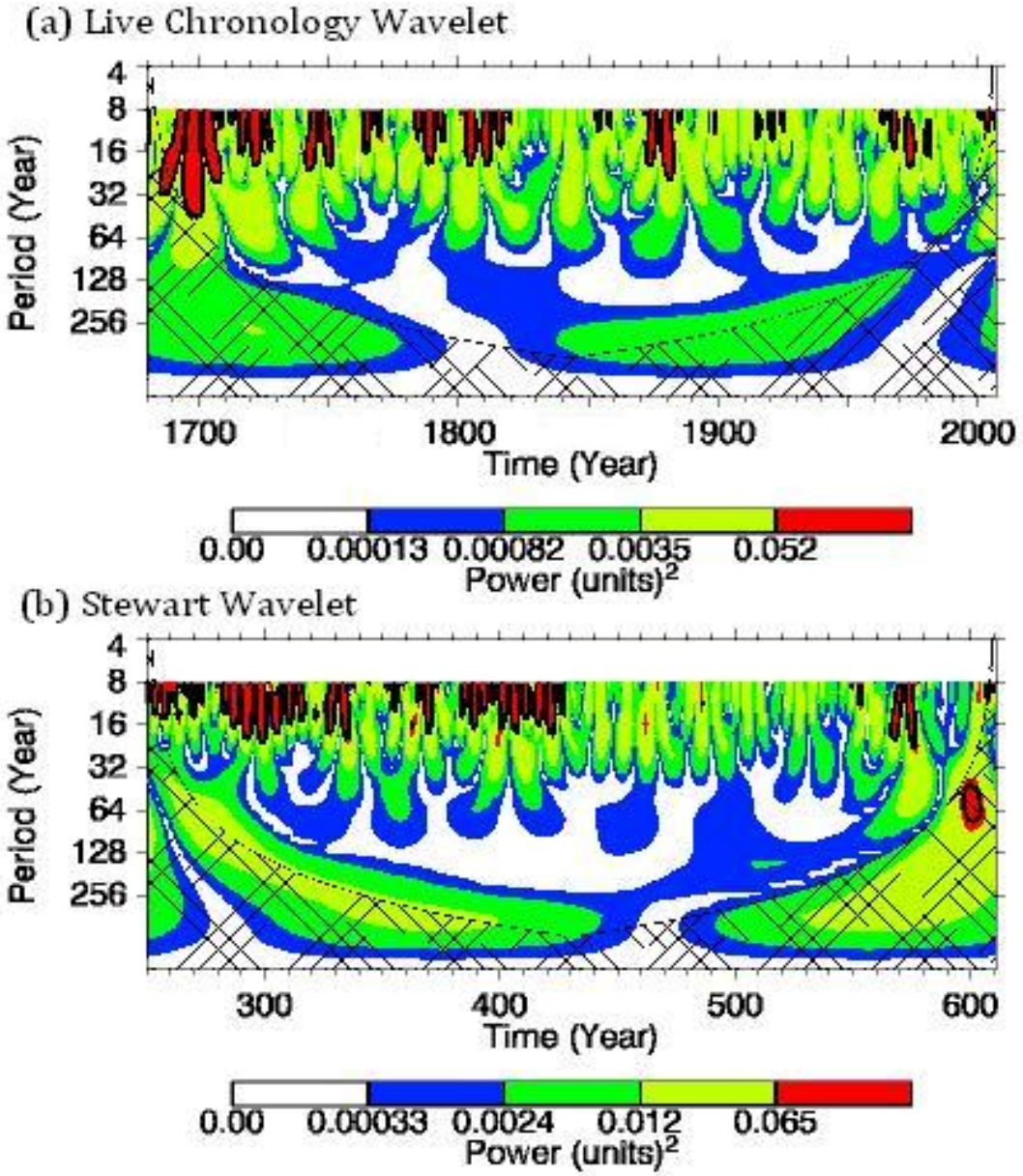

3.23(a), but appears to weaken in the Stewart chronology as the FMA glacier expansion began prior to 460 A.D. (Figure 3.23(b)). A 32-year event thought to be associated with the Pacific Decadal Oscillation (PDO) is prominent within the live chronology; this pattern is more weakly expressed within the FMA chronology after 425 A.D. until after 550 A.D.

The temporal signals retained within the living and subfossil chronologies indicate that climate forcing events originating over the Pacific Ocean have persistently influenced the radial growth of trees in this region. The correspondence of shifts in the character of these relationships over time to the FMA and early-LIA advances documented in this study hints at the role that La Niña events may have in generating positive glacier mass balance states and glacier advances over the last two millennium (c.f. Villalba *et al.* 2001; Watson *et al.* 2006). Documentation of enhanced PDO activity after 550 A.D. and in the late-LIA period (1800-1900 A.D.), likely to be associated with higher winter precipitation and cooler summers, may similarly reflect significant intervals of positive mass balance (Bitz and Battisti 1999; Lewis and Smith 2004). Observation of the persistent influence of phase pairings of La Niña/negative PDO years on glacier mass balance over the last two millennium confirm the findings of shorter duration studies elsewhere in the western Canadian Cordillera (Watson *et al.* 2006).

Proxy evidence of this relationship comes from western hemlock (*Tsuga heterophylla* [Raf.] Sarg.) pollen deposited in Pyramid Lake in the Cassiar Mountains of BC and the Yukon Territory (Spooner *et al.* 2003). Increases in the influx of the percentage of coastal pollen type beginning ca. 1500 yr BP is

interpreted to be a consequence of changes in regional air-mass circulation patterns that brought cooler and wetter weather to PNA (Overland *et al.* 1999). If this interpretation is correct, the FMA advances recorded throughout PNA at this time may be associated with persistence of deeper Aleutian Low pressure systems (Trenberth 1990).

3.8 Summary

Glaciers flowing from the Cambria Icefield in northwestern B.C. have receded and down-wasted significantly over the last 60 years. Investigations completed in the recently deglaciated forefields of South Flat and White glaciers led to the discovery of two late Holocene intervals of glacier expansion.

Dendroglaciological evidence from the White Glacier forefield describes an FMA ice front advance from 486 to 664 A.D. Expansion and thickening of White Glacier by 765 A.D. resulted in creation of an ice damned lake in South Flat valley that may have persisted until 1080 A.D. after which the lake drained, before refilling in the early-LIA. Sometime after 1300 A.D. South Flat and White glaciers became confluent and flowed over the valley side toward White Lake. The characteristics of the site and the preservation of FMA-aged deposits indicate that the two glaciers remained confluent throughout the remainder of the LIA, only separating following terminal retreat early in the 20th Century.

The late Holocene glacial history of South Flat and White glaciers appears synchronous with those of the other glaciers in northern portion of PNA. An assessment of living and subfossil tree ring records from the Cambria Icefield area

was used to infer the climate forcing mechanisms that resulted in the documented FMA and early-LIA advances. Persistent temporal relationships to the ENSO and PDO climate indices are reflective of the strong maritime influence that the Pacific Ocean has on glacier mass balance regimes in the region. Whereas decadal-interdecadal shifts in these relationships result in ice front fluctuations, it seems likely that sustained events like the FMA arose following pronounced reconfigurations of regional air-mass circulation patterns.

Chapter 4

Conclusions

The overall goal of this research was to investigate the late Holocene paleoenvironmental history at White and South Flat glaciers. This was achieved by employing dendrochronological techniques to thus better understand the region's climate and glacial history.

The dendroclimatological objective of this research was to develop a proxy record of climate change from tree ring-width chronologies collected in the vicinity of the Cambria and Todd Icefields (Chapter 2). With this information, an annually resolved proxy record of recent (327 years) climate change was developed. The three stands, located along a 35 km transect cross dated allowing for the development of a network of mountain hemlock chronologies. A master chronology for the region was constructed spanning 409 years (1596 to 2007 A.D.). Correlation analyses show that the radial growth of the master regional chronology examined was sensitive to the mean June-July-August (JJA) air temperature. Due to limited sample depth within the oldest trees, a proxy record of mean JJA air temperature was reconstructed, spanning 307 years (1680 to 2007 A.D.). The reconstruction highlights warm and cool intervals that are synchronous to those derived from other paleoenvironmental research in this region. The record also confirmed the influence of the PDO and ENSO on the climate regime of the region.

The findings of this research also emphasize the complexity of the relationship between climate and radial growth in mountain hemlock trees.

Previous research has highlighted a correlation between a number of climatic variables that mountain hemlock trees respond to in a variety of locations. The three stands used in the study were south-east facing on the windward side of the Coast mountains, which is hypothesized reflect either a physiological response to increased rates of photosynthesis during warm summers (i.e., Kramer and Kozlowski 1960) or, alternatively, an indirect response resulting from accelerated melting of the seasonal snowpack during warm summers. The outcome is an extension of the growing season and potentially an extension of the period over which cambium is produced. Furthermore, the tree-growth correlated more significantly with Dease Lake, a high elevation climate station located 260 km away from the study site on the windward side of the Coast Mountains. This site showed much less variance in annual temperature and precipitation means compared to the low-lying climate station at Stewart Airport, around 35 km west of the study area. Higher elevation and east-facing slopes are drier and therefore this allowed for mean JJA air temperatures to greatly influence growth.

The dendroglaciological objective of the study was to use radiocarbon dating and dendrochronological cross-dating techniques to reconstruct the Holocene behavior of White and South Flat glaciers (Chapter 3). The findings indicate a complex history of glacier expansion, especially between the interaction of White and South Flat glaciers. A reconstruction of a First Millennial Advance phase and the history of late-Little Ice Age glacier expansion were completed through the analysis of sediment units, geomorphological features and buried wood discovered in the forefield of White Glacier and the South Flat valley.

Radiocarbon dates indicate that one of the floating chronologies represents living trees that were killed during an advance at White Glacier cumulating around 600 A.D. There was also evidence from glacially killed trees at two LIA advances around 1200 and 1400 A.D. Based on this evidence, it appears these glaciers have responding similarly to other glaciers in the region, yet evidence for some known advances (i.e. the Tiedermann advance; Jackson *et al.* 2008) was not found at this site.

The temporal signals retained within the living and subfossil chronologies indicate that climate forcing events originating over the Pacific Ocean have persistently influenced the radial growth of trees in this region. Analysis of the low and high frequency variability within a live chronology and FMA chronology highlight temporal rhythms in climate conditions retained within these subfossil and living chronologies.

References

Allen, S.M., and Smith, D.J. 2007. Late Holocene glacial activity of Bridge Glacier, British Columbia Coast Mountains. *Canadian Journal of Earth Sciences* 44:1753-1773.

Barclay, D.J., Barclay, J.L., Calkin, P.E., and Wiles, G. C. 2006. A revised and extended Holocene glacial history of Icy Bay, southern Alaska, U.S.A. *Arctic, Antarctic and Alpine Research* 38:153-162

Barclay, D.J., Wiles, G.C., and Calkin, P.E. 2009. Holocene glacier fluctuations in Alaska. *Quaternary Sciences Review* 28:2034-2048.

Biondi, E., and Swetnam, T.W. 1987. Box-Jenkins models of forest interior tree-ring chronologies. *Tree-Ring Bulletin* 47:71-95.

Biondi, F., and Waikul, K. 2004. DENDROCLIM2002: A C++ program for statistical calibration of climate signals in tree-ring chronologies. *Computers and Geosciences* 30:303-311.

Bitz, C.C., and Battisti, D.S. 1999. Interannual to decadal variability in climate and the glacier mass balance in Washington, western Canada, and Alaska. *Journal of Climate* 12:3181-3196.

Black, B.A., Copenheaver, C.A., Frank, D.C., Stuckey, M.J., and Kormanyos, R. E. 2009. Multi-proxy reconstructions of northeastern Pacific sea surface temperature data from trees and Pacific geoduck. *Palaeogeography, Palaeoclimatology, Palaeoecology* 278:40-47.

Bonsal, B., Shabbar, R.A., and Higuchi, K. 2001. Impacts of low frequency variability modes on Canadian winter temperature. *International Journal of Climatology* 21: 95-108.

Briffa, K.R., Osborn, T.J., and Schweingruber F.H. 2004. Large-scale temperature inferences from tree rings: A review. *Global Planetary Change* 40:11-26.

Brubaker, L.B. 1980. Spatial patterns of tree growth anomalies in the Pacific Northwest. *Ecology* 61:798-807.

Clague, J.J. 1989. Quaternary geology of the Canadian Cordillera. *In* Quaternary Geology of Canada and Greenland, *Edited by* Fulton, R.J. Geological Survey of Canada, Geology of Canada. 1:15-96.

Clague, J.J., and Mathews, W.H. 1992. The sedimentary record and Neoglacial history of Tide Lake, northwestern British Columbia. *Canadian Journal of Earth Sciences* 29:2383-2396.

Clague, J.J., and Mathewes, R.W. 1996. Neoglaciation, glacier-dammed lakes, and vegetation change in northwestern British Columbia, Canada. *Arctic and Alpine Research* 28:10-24.

Clague, J.J., and James, T.S. 2002. History and isostatic effects of the last ice sheet in southern British Columbia. *Quaternary Science Reviews* 21:71-87.

Cook, E.R. 1985. A time-series analysis approach to tree-ring standardization. Ph.D. thesis, University of Arizona, Tucson, Arizona.

Cook, E.R., and Peters, K. 1981. The smoothing spline: a new approach to standardizing forest interior tree-ring width series for dendrochronology. *Tree-Ring Bulletin* 41:45-53.

Cook, E.R., and Holmes, R.L. 1986. Guide for computer program ARSTAN (Adapted from Users Manual for Program ARSTAN). *In* Tree-Ring Chronologies of Western North America: California, Eastern Oregon, and Northern Great Basin. *Edited by* Holmes, R.L. and Fritts, H.C. University of Arizona Laboratory of Tree Ring Research, Tucson, Arizona.

Cook, E.R., and Kairiukstis, L. 1990. Methods of Dendrochronology: Applications in the Environmental Sciences, Kluwer Academy, Norwell, Massachusetts.

Cook, E.R., Shiyatov, S., and Mazepa, V. 1990. Estimating the mean chronology. *In* Methods of Dendrochronology: Applications in the Environmental Sciences. *Edited by* E.R. Cook and L.A. Kairiukstis. Kluwer Academic Publishers, Boston, Massachusetts. 394 pp.

Cook, E.R., Woodhouse, C.A., Eakin, C.M., Meko, D.M., and Stahle. D.W. 2004. Long-term aridity changes in the western United States. *Science* 306:1015-1018.

D'Arrigo, R.D., Jacoby, G.C., Free, M., and Robock, A. 1999. Northern hemisphere annual to decadal temperature variability for the past three centuries: Tree-ring and model estimates. *Climatic Change* 42:663-675.

D'Arrigo, R.D., Mashig, E., Frank, D., Wilson, R., and Jacoby, G. 2005. Temperature variability over the past millennium inferred from Northwestern Alaska tree rings. *Climate Dynamics* 24:227-236.

Denton G. H., and Stuiver M. 1966. Neoglacial chronology, North Eastern St. Elias Mountains, Canada. *American Journal of Science* 264:577-599.

Desloges, J.R., and Ryder, J.M. 1990. Neoglacial history of the Coast Mountains near Bella Coola, British Columbia. *Canadian Journal of Earth Sciences* 27:281-290.

Ettl G.J., and Peterson D.L. 1995. Growth response of subalpine fir (*Abies lasiocarpa*) to climate in the Olympic Mountains, Washington, USA. *Global Change Biology* 1:213-230.

Field, W.O. 1926. The Fairweather Range: Mountaineering and glacier studies. *Appalachia* 16:460-472.

Fritts, H.C. 1976. Tree Rings and Climate. Academic Press, New York.

Fulton, R.J. 1984. Quaternary Glaciation, Canadian Cordillera. *In* Quaternary stratigraphy in Canada – a Canadian contribution to IGCP Project 24. *Edited by* Fulton, R.J. *Geological Survey of Canada,* Paper 84-10.

Gedalof, Z. 2002. Low Frequency Climate variability in the Northeast Pacific Interpreted from the annual growth-rings of mountain hemlock. MSc thesis, University of Victoria, Victoria, British Columbia.

Gedalof, Z., and Smith, D.J. 2001a. Dendroclimatic response of mountain hemlock (*Tsuga mertensiana*) in Pacific North America. *Canadian Journal of Forest Research* 31:322-332.

Gedalof, Z., and Smith, D.J. 2001b. Interdecadal climate variability and regime-scale shifts in Pacific North America. *Geophysical Research Letters* 28:1515-1518.

Graumlich, L.J., and Brubaker, L.B. 1986. Reconstruction of annual temperature (1590-1976) for Longmire, Washington, derived from tree-rings. *Quaternary Research* 25:223-234.

Grissino-Mayer, H.D. 2001. Evaluating cross-dating accuracy: A manual and tutorial for the computer program COFECHA. *Tree-Ring Research* 57:205-221.

Grove, J.M. 1973. Detailed geological studies in the Stewart complex, northwestern British Columbia. PhD Thesis. McGill University, Montreal, Quebec.

Grove, J.M. 1988. The Little Ice Age. Methuen, London.

Grudd, H., Briffa, K.R., Karlén, W., Bartholin, T.S., Jones, P.D., and Kromer, B. 2002. A 7400-year tree-ring chronology in northern Swedish Lapland: natural climatic variability expressed on annual to millenial timescales. *The Holocene* 12**:**657-665.

Guay, R., Gagnon, R., and Morin, H. 1992. MacDENDRO, a new automatic and interactive tree ring measurement system based on image processing. *In* Tree Rings and Environment: Proceedings of the International Dendrochronological

Symposium, Ystad, Sweden, 3–9 September 1990, Lundqua Report. Lund University. pp 128-129.

Hansen, J., and Lebedeff, S. 1987. Global trends of measured surface air temperature. *Journal of Geophysical Research* 92:345-372.

Haspel, R., Osborn, J., and Spooner, I. 2005. Neoglacial deposits of Bear River Glacier, northern Coast Ranges, British Columbia. *In* Proceedings, Annual Meeting of the Western Division, Canadian Association of Geographers, University of Lethbridge, Lethbridge, AB. 11-13 March 2005.

Hoadley, R.B. 1990. Identifying Wood: Accurate Results with Simple Tools. Newtown, Connecticut. Taunton Press.

Holmes, R.L., Adams, R.K., and Fritts, H.C. 1986. Tree- ring chronologies of western North America: California, eastern Oregon, and northern Great Basin. Laboratory of Tree-Ring Research, Chronology Series VI. University of Arizona Press, Tucson, Arizona, USA.

Hughes, M.K. 2002. Dendrochronology in climatology - the state of the art. *Dendrochronologia* 20:95-116.

Jackson, S.I., Laxton, S.C., and Smith, D.J., 2008. Dendroglaciological evidence for Holocene glacial advances in the Todd Icefield area, Northern British Columbia Coast Mountains. *Canadian Journal of Earth Sciences* 45:83-98.

Johnson, A.N., Wiles, G.C., and Frank, D.C. 1997. Three millennia of glacial fluctuations from Beare Glacier, eastern Gulf of Alaska. *Geological Society of America Abstracts with Programs* 29:23.

Koch, J., Clague, J.J., and Osborn, G.D. 2007. Glacier fluctuations during the past millennium in Garibaldi Provincial Park, southern Coast Mountains, British Columbia. *Canadian Journal of Earth Sciences* 44:1215-1233.

Koehler, L., and Smith, D.J. *in press*. Late-Holocene glacial activity in Manatee Valley, southern Coast Mountains, British Columbia, Canada. *Canadian Journal of Earth Sciences*

Klinka, K., Pojar, J., and Meidinger. D.V. 1991. Revision of biogeoclimatic units of coastal British Columbia. *Northwest Science*. 65:32-47.

Krajina V. 1969. Ecology of forest trees in British Columbia. *Ecology of Western North America* 2:1-146.

Kramer, P.J., and Kozlowski, T.T. 1960. Physiology of Trees. McGraw-Hill Book Company, New York.

Larocque, S.J., and Smith, D.J. 2003. Little Ice Age glacial activity in the Mt. Waddington area, British Columbia Coast Mountains, Canada. *Canadian Journal of Earth Sciences* 40:1413-1436.

Larocque, S.J., and Smith, D.J. 2004. Calibrated *Rhizocarpon geographicum* growth curve for the Mount Waddington area, British Columbia Coast Mountains, Canada. *Arctic, Antarctic and Alpine Research* 36:407-418.

Larocque, S.J., and Smith, D.J. 2005. Little Ice Age proxy glacier mass balance records reconstructed from tree rings in the Mt. Waddington area, British Columbia Coast Mountains, Canada. *The Holocene* 15:748-757.

Laroque, C.P., and Smith, D.J. 2001. A 900-year record of Pacific Decadal Oscillations in Pacific North America. Annual Meeting of Western Division of the Canadian Association of Geographers-Abstracts. March 8-10, 2001. University of Calgary, Alberta.

Laxton, S. 2005. Dendroglaciological reconstruction of late Holocene glacier activity at Todd Glacier, Boundary Range, northwestern British Columbia Coast Mountains. MSc thesis, University of Victoria, Victoria, British Columbia.

Laxton, S., Smith, D.J., Desloges, J.R., and Day, A. 2003: Late-Holocene history of Fyles Glacier, Coast Mountains, British Columbia. Abstracts of the Joint Meeting of the Association of Canadian Map Libraries and Archives, Canadian Association of Geographers, Canadian Cartographic Association, and Canadian Regional Science Association 2003. Victoria, British Columbia.

LeBlanc, D., and Terrell, M. 2001. Dendroclimatic analyses using the Thornthwaite-mather-type evapotranspiration models: a bridge between dendroecology and forest simulation models. *Tree-Ring Research* 57:55-66.

Lewis, D.H., and Smith, D.J. 2004. Dendroglaciological mass balance reconstruction, Strathcona Provincial Park, Vancouver Island, British Columbia, Canada. *Arctic, Antarctic and Alpine Research* 36:598-606.

Lewis, D.H., and Smith, D.J. 2005. Dendroglaciological evidence of late Holocene glacier activity at Forrest Kerr Glacier, Andrei Icefield, northern British Columbia Coast Mountains. *In* Proceedings Annual Meeting of the Canadian Association of Geographer.

Luckman, B.H. 1986. Reconstruction of Little Ice Age events in the Canadian Rocky Mountains. *Géographie physique et Quaternaire* 40:17-28.

Luckman, B.H. 1995. Calendar-dated, early 'Little Ice Age' glacier advance at Robson Glacier, British Columbia, Canada. *The Holocene* 5:149-59.

Luckman, B.H. 1998. Dendroglaciologie dans les Rocheuses du Canada. *Géographie physique et Quaternaire* 52:139-151.

Luckman, B.H. 2007. Tree Rings as Temperature Proxies. Gussow-Nuna Geoscience Conference. October 20-23, Banff, Alberta.

Luckman, B.H., and Villalba, R. 2001 Assessing synchroneity of glacier fluctuations in the western cordillera of the Americas during the last millennium. *In* Interhemispheric climate linkages. *Edited by* V. Markgraf. Academic Press, New York,. 119–140.

McConnell, R.G. 1913. Portions of Portland Canal and Skeena Mining Divisions, Skeena District, B. C., Geological Survey of Canada Memoir 32: Geological Survey No. 25, Ottawa.

Mann, M.E., Bradley, R.S., and Hughes, M.K. 1999. Northern Hemisphere temperatures during the past millennium: Inferences, uncertainties, and limitations. *Geophysical Research Letters* 26:759–762.

Mantua, N.J., Hare, S.R., Zhang, Y., Wallace, J.M., and Francis, R.C. 1997. A Pacific interdecadal climate oscillation with impacts on salmon production. *Bulletin of the American Meteorological Society* 78:1069-1079.

Mantua, N.J., and Hare, S.R. 2002. The Pacific Decadal Oscillation. *Journal of Oceanography* 58:35-44.

Mathews, W.H. 1965. Two self-dumping ice-dammed lakes in British Columbia. *Geographical Review* 55:46-52.

Means, J.E. 1990. *Tsuga mertensiana* (Bong.) Carr. Mountain hemlock. *In* Silvics of North America. Vol. 2. *Edited by* R.M. Burns and B.H. Honkala. Washington, *U.S. Department of Agriculture: Agriculture Handbook* 1:623–634.

Meidinger, D., and Pojar, J. 1991. Ecosystems of British Columbia. British Columbia Ministry of Forests, Victoria, British Columbia. Special Report No. 6.

Menounos, B., Koch, J., Osborn, G., Clague, J.J., and Mazzucchi, D. 2004. Early Holocene glacier advance, southern Coast Mountains, British Columbia, Canada. *Quaternary Science Reviews* 23:1545-1550.

Menounos, B., Osborn, G., Clague, J.J., and Luckman, B.H. 2009. Latest Pleistocene and

Holocene glacier fluctuations in western Canada. *Quaternary Science Reviews* 28:2049-2074.

van Oldenborgh G.J., and Burgers, G. 2005. Searching for decadal variations in ENSO precipitation teleconnections. *Geophysical Research Letters* 32.

Osborn, J., Menounos, B., Clague, J.J., Koch,J., and Vallis, V. 2007. Multi-proxy record of Holocene glacial history of the Spearhead and Fitzsimmons ranges, southern Coast Mountains. *Quaternary Science Reviews* 26:479-493.

Overland, J.E., Adams, J.M., and Bond, N.A. 1999. Decadal variability of the Aleutian Low and its relation to high-latitude circulation. *Journal of Climate* 12:1542-1548.

Parish, R., and Antos, J.A. 2006. Slow growth, long-lived trees, and minimal disturbance characterize the dynamics of an ancient, montane forest in coastal British Columbia. *Canadian Journal of Forest Research* 36:2826-2838.

Penrose, K.A. 2007. Radial-growth response of mountain hemlock (*Tsuga mertensiana*) trees to climate variations along a longitudinal transect, northwestern British Columbia, Canada. MSc thesis, University of Victoria, Victoria, British Columbia.

Peterson, D.W., and Peterson, D.L. 2001. Mountain hemlock growth responds to climatic variability at annual and decadal scales. *Ecology* 82:3330-3345.

Pojar, J., Klinka, K., and Meidinger, D.V. 1987. Biogeoclimatic ecosystem classification in British Columbia. *Forest Ecology Management* 22:119-154.

Rasmusson, E.M., and Wallace, J.M. 1983. Meterological aspects of the El Nino/Southern Oscillation. *Science* 222:1195-202.

Reyes, A.V., and Clague, J.J. 2004. Stratigraphic evidence for multiple Holocene advances of Lillooet Glacier, southern Coast Mountains, British Columbia. *Canadian Journal of Earth Sciences* 41:903-918.

Reyes, A.V., Wiles, G.C., Smith, D.J., Barclay, D.J., Allen, S., Jackson, S., Larocque, S., Laxton, S., Lewis, D., Calkin, P.E., and Clague, J.J. 2006. Expansion of alpine glaciers in Pacific North America in the first millennium AD. *Geology* 34:57-60.

Ryder, J.M. 1987. Neoglacial history of the Stikine-Iskut area, northern Coast Mountains, British Columbia. *Canadian Journal of Earth Sciences* 24:1294–1301.

Ryder, J.M., and Thomson, B. 1986. Neoglaciation in the southern Coast Mountains of British Columbia" chronology prior to the late neoglacial maximum. *Canadian Journal of Earth and Ocean Sciences* 23:273-287.

Smith, D.J., and Laroque, C.P. 1998. Mountain hemlock growth dynamics on Vancouver Island. *Northwest Science* 72:67-70.

Smith, D.J., and Desloges, J.R. 2000. Little Ice Age history of Tzeetsaytsul Glacier, Tweedsmuir Provincial Park, British Columbia. *Géographie physique et Quaternaire* 54:135-141.

Smith, D.J., and Lewis, D. 2007a. Dendroglaciology. *In* Encyclopedia of Quaternary Science. *Edited by*: S.A. Elias. Elsevier Scientific. Amsterdam, The Netherlands. 2:986-994.

Smith, D.J., and Lewis, D. 2007b. Dendrochronology. *In* Encyclopedia of Quaternary Science. *Edited by*: S.A. Elias. Elsevier Scientific. Amsterdam, The Netherlands. 1:459-465.

Spooner, I.S., Barnes, S., Baltzer, K.B., Raeside, R., Osborn G.D., and Mazzucchi, D. 2003. The impact of air mass circulation dynamics on Late Holocene paleoclimate in northwestern North America. *Quaternary International* 108:77-83.

Spooner, I., Haspel, R., and Osborn, G.D. 2005. Holocene history of Bear River Glacier, northern Coast Ranges, British Columbia. *In* Water, Ice, Land, and Life: The Quaternary Interface. Canadian Quaternary Association, University of Manitoba, Winnipeg, Manitoba. A87.

Stokes, M.A., and Smiley, T.L. 1968. Tree-Ring Dating. The University of Chicago Press, Chicago, Ill.

Swetnam, T., and Betancourt, J. 1998. Mesoscale disturbance and ecological response to decadal climatic variability in the American Southwest. *Journal of Climate* 11:3128-3147.

Torrence, C., and Compo, G.C. 1998. A practical guide to wavelet analysis. *Bulletin of the American Meteorological Society* 79:61-78.

Tourre, Y.M., Rajagopalan, B., Kushnir, Y., Barlow, M., and White W.B. 2001. Patterns of coherent decadal and interdecadal climate signals in the Pacific Basin during the 20th Century. *Geophysical Research Letters* 28:2069-2072.

Trenberth, K.E. 1990. Recent observed interdecadal climate changes in the northern hemisphere. *Bulletin of the American Meteorological Society* 71:988-993.

Villalba, R., D'Arrigo, R.D., Cook, E.R., Wiles, G., and Jacoby G.C. 2001. Decadal-scale climatic variability along the extra-tropical western coast of the Americas over past centuries inferred from tree-ring records, *In* Interhemispheric Climate Linkages. *Edited by* V. Markgraf, Cambridge University Press, Cambridge, UK.

Visser, H., Buntgen, U., D'Arrigo, R., and Petersen, A.C., 2010. Detecting instabilities in tree-ring proxy calibration. *Climate Past Discussion* 6:225–255.

Walker, I.R., and Pellatt, M.G. 2003. Climate change in coastal British Columbia -a paleoenvironmental perspective. *Canadian Water Resources Journal* 28:531-566.

Watson, E., and Luckman, B.H. 2004. Tree-ring estimates of mass balance at Peyto Glacier for the last three centuries. *Quaternary Research* 62:9-18.

Watson, E., Luckman, B.H., and Yu, B. 2006. Long-term relationships between reconstructed seasonal mass balance at Peyto Glacier, Canada and Pacific variability. *The Holocene* 16:783-790.

Wigley, T.M.L., Briffa, K.R., and Jones, P.D. 1984. On the average value of correlated time series, with applications in dendroclimatology and hydrometeorology. *Journal of Applied Meteorology* 23:201-213.

Wiles, G.C., D'Arrigo, R., and Jacoby, G.C. 1998. Gulf of Alaska atmosphere ocean variability over recent centuries inferred from coastal tree-ring records. *Climate Change* 38:289-306.

Wiles, G.C., Barclay, D.J., Calkin, P.E., and Lowell, T.V. 2008. Century to millennial-scale temperature variations for the last two thousand years indicated from glacial geologic Records of Southern Alaska. *Global and Planetary Change* 60:115–125.

Wilson, R.J.S. and Luckman B.H. 2002. Tree-ring reconstruction of maximum and minimum temperatures and the diurnal temperature range in British Columbia, Canada. *Dendrochronologia* 20:257–268.